

**We thank the reviewer for helpful and constructive comments.**

*China is experiencing the low visibility and serious air pollution in large regional scale during last few years. January 2103 was the worst month when the heavy air pollution episodes last almost whole month and covered the most of China. The MS investigated the episode happened in January 2013 and study the feedback of aerosol and meteorological variables. It gives a highlight to understand the pollution process and it represents a substantial contribution to scientific community. However there are a few questions needed to be revised.*

*1. "Fog-haze" was used in the title, it is important to define what is the fog-haze day.*

**Reply:**

We thank the reviewer for this constructive comment.

The "severe fog-haze event" in the title refers to the period of 10~15 January when the aerosol concentration was very high and the atmospheric visibility was extremely low. Now we make it more clear in the manuscript:

We revise the sentence at Page 1094 Line 5 to "The numerical experiments are performed for the period 2–26 January 2013, during which a severe fog-haze event (10–15 January 2013) occurred with the simulated maximum hourly surface PM<sub>2.5</sub> concentration of ~600 ug m<sup>-3</sup>, minimum atmospheric visibility of ~0.3 km and 10–100 hours of simulated hourly surface PM<sub>2.5</sub> concentration above 300 ug m<sup>-3</sup> over NCP."

We revise the sentence at Page 1096 Line 3~4 to "During 10–15 January 2013, extremely severe fog-haze occurred over the NCP, especially over Beijing, Tianjin, and south of Hebei Province with very high aerosol concentration and extremely low atmospheric visibility."

We also revise the sentence at Page 1106 Line 10 to "In this section, the aerosol radiative forcing (ARF) and its impacts on surface energy, temperature, RH, atmospheric stability, wind, and PBLH during the fog-haze period (10–15 January) with the simulated maximum surface PM<sub>2.5</sub> concentration of ~600 ug m<sup>-3</sup>, minimum atmospheric visibility of ~0.3 km and 10–100 hours of simulated hourly surface PM<sub>2.5</sub> concentration above 300 ug m<sup>-3</sup> over NCP are presented."

*2. Some figures are not clear, especially in Fig. 1 and Fig. 2.*

**Reply:**

We thank the reviewer for this helpful comment.

As the terrain height is not mentioned in the manuscript, now we delete the distribution of terrain height in Fig. 1 to make Fig. 1 more clear. We also check Fig. 2 and other figures to make them more clear.

**We thank the reviewer for helpful and constructive comments.**

*The Gao et al. article presents results from the WRF-Chem model run for a particularly severe, regional-scale air pollution episode over the North China Plain in January 2013. The authors compare two simulations from the 'on-line' aerosol/chemistry model: one allowing for feedbacks between the aerosols and chemical fields on the meteorological fields and a second simulation where these interactions are not allowed. There is a growing body of research investigating the effects of aerosols on the shorter term evolution of the atmosphere and this research adds to that by investigating the influence of aerosol feedbacks on near-surface aerosol concentrations through modifications to the meteorology during this particularly intense pollution episode.*

*While the methodology and conclusions of the study are logical and well-founded, the one facet of the study that does appear to be weak is the assessment of the model predictions of aerosol amounts and related quantities such as aerosol optical depth against observations. Surface concentrations of PM<sub>2.5</sub> are compared against observations for four stations, though all of these stations are in the vicinity of Beijing and are removed from the region with the highest aerosol amounts, judging from the spatial distributions presented in Figure 7. Additional comparisons are shown for aerosol optical depth (AOD) from sunphotometer measurements and point measurements of AOD from MODIS for most of these same stations around Beijing. The only observations further away from the region of Beijing are visibility measurements at Shijiazhuang and Baoding.*

*Certainly nothing can be done about sparse observations, but looking at the observations presented in Che et al. (Atmos. Chem. Phys., 14, 2125-2138,*

2014) for this same pollution episode there are sunphotometer measurements of AOD at Huimin, about 300 km south of Beijing and within the BTH region used for spatial averaging of quantities presented in several of the figures.

While Wang et al. (*Atmos. Envir.*, 89, 807-815, 2014) present maps of MODIS AOD for this same period, which would help extend the spatial coverage of the comparison of model output with observations. Additionally, Wang et al. use CALIPSO cross-sections of extinction to show that much of the aerosol is within 1 km of the surface for this episode. The vertical extent of the aerosols would be an important quantity to assess for the modeling presented here.

The modeling results and analysis of the 'positive feedbacks' of aerosols on the aerosol concentrations near the surface for this globally significant region are fascinating, however the lack of a thorough comparison with observations makes it difficult to assess how accurate the estimate of the magnitude of these effects are. I will note that the comparisons for Xianghe and Tianjin, the two stations furthest to the south of Beijing with PM<sub>2.5</sub> observations both show substantial over-estimations of PM<sub>2.5</sub> concentration on the order of 30 to 60%. How the overestimations at Xianghe and Tianjin may be related to the model estimations of larger aerosol effects further to the south and west is an open question. A comprehensive (as possible) comparison of model results with different observations would help to strengthen the quantitative estimates of the effects of aerosols on the meteorology during this episode.

**Reply:**

We thank the reviewer for this constructive comment. The evaluation of model results is very important. Now we make the revisions as follows

according to the reviewer's comments:

First, following the reviewer's comment, now we cite the observation data of AOD at Huimin site in Che et al. (2014) and compare the corresponding model results from the EXP-CTL case with it. We add the comparison in Figure 5 and Table 1. The comparison shows that model can reproduce the variation of AOD at Huimin site with the *correlation coefficients* of 0.74 but may underestimate it with the *mean bias* of -0.22. We also add the following revision or discussion to the manuscript.

Page 1102 Line 8: "We also use the AOD data at Huimin site (37.48 °N, 117.53 °E, 11.7 m.s.l.) from Che et al. (2014) which is collected from the China Aerosol Remote Sensing Network (CARSNET) and were processed using the ASTPwin software offered by Cimel Ltd. Co (Che et al., 2009a). This site is denoted as a cross in Fig.1."

Page 1106 Line 3: "the R values between the simulated and observed AODs from AERONET are 0.59, 0.99, 0.60 and 0.74 for the BJ, XL, XH and Huimin sites, respectively. The AOD from MODIS is much higher than that from AERONET, indicating that the AOD may be overestimated by MODIS. The modeled averaged AOD is higher at XH and lower at XL, consistent with the surface PM<sub>2.5</sub> concentration at these two sites (Fig. 3). Although model underestimates AOD at Huimin site with the MB of -0.22, both observation and model result show that the AOD at Huimin site is highest among the four sites. Considering the location of Huimin site in Figure 1, this indicates that model can reproduce the more serious pollution to the south of Beijing province."

Secondly, following the reviewer's comment, now we compare the daily distribution of AOD at 550nm at 13:00 from MODIS retrievals and the

corresponding model results from the EXP-CTL case from 6~17 January 2013 over the North China Plain. The figures are presented in the supplement file and we add the following discussion.

"Figure S1 is the daily distribution of AOD at 550nm at 13:00 from MODIS observations and the corresponding model results from the EXP-CTL case from 6~17 January 2013 over the North China Plain (NCP). In Fig. S1, comparing with MODIS retrievals, the model may underestimate AOD, although there is many missing data from MODIS retrievals. Seen in Fig. 2(a), MODIS tends to overestimates AOD comparing with AERONET. Some previous studies (Ge et al., 2010; Prasad and Singh, 2007, Diner et al., 2005; Li et al., 2009, Wu et al., 2014) also indicated that MODIS retrieved AOD significantly depended on both the aerosol type and the underlying surface type and had large uncertainties. Even though model results could reproduce the more pollutants over the south part of Hebei Province and the evolution of AOD values during the fog-haze period: the event starts from 10 January, when the AOD increases a lot over Beijing, Tianjin and Hebei province. After that, the value of AOD continues to increase during 11 January. Both model results and MODIS retrievals show the decrease of AOD on 12 January and the increase on 13 January. On 14 January, AOD begins to decrease over Beijing but maintains a high value over south of Hebei province."

Thirdly, following the reviewer's comment, now we compare the altitude-orbit cross-section of 532 nm extinction coefficient from CALIPSO and the modeled aerosol extinction coefficient at 532nm from EXP\_CTL at 10~15 January, present the figures in the supplement file and add the following discussion.

"The Cloud-Aerosol Lidar with Orthogonal Polarization (CALIOP) onboard the Cloud-Aerosol Lidar and Infrared Pathfinder Satellite Observations (CALIPSO) provides aerosol vertically resolved extinction and depolarization ratio (Winker et al., 2007; Huang et al., 2007). CALIPSO 532 nm extinction coefficient (Winker et al., 2009) is used to evaluate model results. The horizontal resolution is 5 km and the vertical resolution is 60 m below and 180 m above 20 km, respectively. Figure S2 is the altitude-orbit cross-section of 532 nm aerosol extinction coefficient from CALIPSO and the modeled aerosol extinction coefficient at 532nm from EXP\_CTL at 02:00 11 January, 13:00 11 January, 02:00 13 January, 13:00 13 January, 02:00 15 January and 13:00 15 January (local time). The model results are sampled at the time and location of CALIPSO orbit. The simulated aerosol extinction coefficient at 532nm is calculated by using the default output AOD and Angstrom exponent derived from the output AODs at 400nm and 600nm. As seen in Fig. S2, model can capture the vertical distribution and the evolution of aerosol extinction coefficient during the fog-haze period by comparing with CALIPSO retrievals. Both model results and CALIPSO retrievals show that the high value of extinction coefficient is near the surface below 1 km indicating that the particles mainly concentrate below 1 km. Model also reproduces the shift of pollutant from south (between ~32 °N and 34 °N) to north (between 37 °N and 40 °N) from 11 January to 13 January."

Finally, for the overestimations of PM<sub>2.5</sub> concentration at Xianghe and Tianjin mentioned by reviewer, now we add the following discussion to the conclusion part of the manuscript.

"There are uncertainties in this study. The model overestimates PM<sub>2.5</sub> at

Xianghe and Tianjin according to Figure 3. The diurnal variation of  $PM_{2.5}$  at Xianghe and Tianjin from model results and observations shows that the overestimation is basically at night which may relate to the setting of atmospheric boundary layer height at night in the model and also the bias of emission inputted to the model. As the aerosol feedback derived from the aerosol radiative effect mainly has large impacts during daytime, it is noted that the overestimation of  $PM_{2.5}$  may lead to slight overestimation of the aerosol feedback during the pollutant period. Emission with higher resolution may be useful for improving the model performance. The aerosol direct and indirect effect is also very sensitive to the mixing state between scattering aerosols and absorbing aerosols. Moreover, the feedback between aerosol and cloud/meteorological parameters also has large uncertainty. Although aerosol indirect forcing is considered in WRF-Chem, it only includes the aerosol effect on resolved stratiform clouds. With a horizontal resolution of 27 km, convective clouds are still parameterized in the model without explicit cloud microphysics in the convective cloud parameterization that links aerosols to cloud condensation or ice nuclei."

*Other minor comments are given below.*

*Page 1096, Line 15: Consider rewording 'a weak weather system'. Perhaps 'weak synoptic-scale winds' or 'a synoptic scale stagnation'?*

**Reply:**

We thank the reviewer for this helpful comment.

Now we revise "a weak weather system" to "a synoptic scale stagnation".

*Page 1098, Lines 10-17: Here it is stated the MADE/SORGAM is used in*

*WRF-Chem and there are several references to the use of a modal aerosol description. On Page 1099, lines 24-28, it is stated that MOSAIC is used and that it is a sectional model with eight size bins. These two statements conflict and it is not clear which aerosol representation was used.*

**Reply:**

We thank the reviewer for this helpful comment.

We use MOSAIC in this study. Now we delete "MADE/SORGAM (Modal Aerosol Dynamics Model for Europe and Secondary Organic Aerosol Model) and" in the manuscript.

*Page 1100, Lines 1-4: Are the MOZART boundary conditions specific to the period being studied or are they climatological? It should be made clear in the article. Note a spelling error on 'MOZART'.*

**Reply:**

We thank the reviewer for this helpful comment.

The MOZART boundary conditions are specific to the period being studied. Now we revise the sentence to "Both the initial and boundary chemical conditions are from MOZART's (Model for Ozone and Related chemical Tracers) chemical boundary conditions which are specific to the period being studied."

*Page 1103, Line 24: In place of 'nowadays' I would suggest 'present-day'.*

**Reply:**

We thank the reviewer for this helpful comment.

Now we revise "nowadays" to "present-day".

*Page 1106, Line 15: Figure 6a presents the difference in the surface energy*

*budget between the two simulations averaged over the BTH region. There is a lot of focus on the Jan 10-15 episode of extreme PM<sub>2.5</sub> concentrations, but it is not at all apparent that Jan 10-15 was much different than the rest of the month. Do you have any ideas why the average over the BTH region does not show a significantly larger signal for Jan 10-15? From the magnitude of the differences plotted in Figure 6a, I assume these numbers are averaged over the full 24 hours each day. Does it make any difference if only the 09-18 LT times are used?*

**Reply:**

We thank the reviewer for this helpful comment.

The reason is that the surface energy change is also very large on 19 and 21 January. Compared to other periods, e.g. 2~9 January, 16~18 January, 20 January and 22~26 January, the energy change during 10~15 January is much larger. From Figure 3, it can be seen that the aerosol concentration on 19 and 21 January was also very high and comparable to that during 10~15 January. We have tried to use the 09~18 LT for average, it almost did not make any difference which also indicated that it may relate to the higher aerosol concentration on specific date in January (e.g., 19 and 21 January) but not the diurnal change of aerosol concentration.

*Page 1106, Line 17: The reference to 'net radiation (LH+LW+SW+SW)' is not quite accurate because not all of the terms included there are radiation. Perhaps 'net energy flux'?*

**Reply:**

We thank the reviewer for this helpful comment.

Now we revise "net radiation" to "net energy flux" in the manuscript.

*Page 1110, Lines 8-10: What does the statement 'The higher the surface PM<sub>2.5</sub> concentration is, the greater the increase is in the surface PM<sub>2.5</sub> concentration...' refer to? Is it the average differences between Beijing, Tianjin and Hebei, or the temporal behaviour of the differences for each station? If it is the temporal behaviour, the fact that at the time of some of the highest peak concentrations in the EXP\_NOEF simulation there are lower PM<sub>2.5</sub> concentrations in the EXP\_CTL should be acknowledged. I believe this is just a result of the internal variability of the meteorology in the simulations and does not impact any of the conclusions of the paper. However the statement should be clarified.*

**Reply:**

We thank the reviewer for this helpful comment.

"The higher the surface PM<sub>2.5</sub> concentration is, the greater the increase is in the surface PM<sub>2.5</sub> concentration..." refer to the average differences between Beijing, Tianjin and Hebei. Now we revise the sentence to " For the average differences between Beijing, Tianjin and Hebei, the higher the surface PM<sub>2.5</sub> concentration is, the greater the increase is in the surface PM<sub>2.5</sub> concentration produced by unfavorable meteorological conditions."

Page 2 Line 3	Insert "(NCP)"
Page 2 Line 7~9	Insert "with the simulated maximum hourly surface PM <sub>2.5</sub> concentration of ~600 ug m <sup>-3</sup> , minimum atmospheric visibility of ~0.3 km and 10–100 hours of simulated hourly surface PM <sub>2.5</sub> concentration above 300 ug m <sup>-3</sup> over NCP."
Page 2 Line 10	Delete "the"
Page 2 Line 13	Insert "reasonably well" Change "Comparison of modeling result" to "Analysis of model result"
Page 2 Line 14	Change "in the presence and absence of" to "with and without" Insert "shows that"
Page 2 Line 15	Delete "shows that"
Page 2 Line 17	Change "of which the" to "with"
Page 2 Line 18	Delete "occur"
Page 4 Line 5	Change "2009" to "2009b"
Page 5 Line 3	Change "11-14" to "10-15"
Page 5 Line 4	Insert "with very high aerosol concentration and extremely low atmospheric visibility"
Page 5 Line 16	Change "weak weather system" to "synoptic scale stagnation"
Page 8 Line 2~3	Delete "MADE/SORGAM (Modal Aerosol Dynamics Model for Europe and Secondary Organic Aerosol Model) and "
Page 10 Line 1~2	Change "MOAZRT's (Model for OZone and Related chemical Tracers) chemical boundary conditions." to " MOZART's (Model for OZone and Related chemical Tracers) chemical boundary conditions which are specific to the period being studied."
Page10 Line 19~20	Insert "(Lei et al., 2011, Zhang et al., 2009, and He et al., 2012)"
Page 12 Line 15~18	Insert "AOD data at Huimin site (37.48 °N, 117.53 °E, 11.7 m.s.l.) from Che et al. (2014) which is collected from the China Aerosol Remote Sensing Network (CARSNET) and were processed using the ASTPwin software offered by Cimel Ltd. Co (Che

	et al., 2009a) is also used. This site is denoted as a cross in Fig.1."
Page 14 Line 15	Change "nowadays" to "present-day"
Page 17 Line 4	Insert "at BJ, XL, and XH and Che et al. (2014) at Huimin site"
Page 17 Line 5	Delete "at BJ, XL and XH"
Page 17 Line 13~14	Change "and 0.60 for the BJ, XL, and XH sites, respectively" to "0.60 and 0.74 for the BJ, XL, XH and Huimin sites, respectively"
Page 17 Line 16	Change "highest" to "higher"
Page 17 Line 17	Change "lowest" to "lower"
Page 17 Line 18~ Page 18 Line 5	<p>Insert "Although model underestimates AOD at Huimin site with the MB of -0.22, both observation and model result show that the AOD at Huimin site is highest among the four sites. Considering the location of Huimin site in Figure 1, this indicates that model can reproduce the more serious pollution to the south of Beijing province.</p> <p>In addition, in the supplement file, the comparison of AOD from MODIS observations and the corresponding model results shows that model can reproduce the more pollutants over the south part of Hebei Province and the evolution of AOD values; the comparison of aerosol extinction coefficient from Cloud-Aerosol Lidar and Infrared Pathfinder Satellite Observations (CALIPSO) and the modeled aerosol extinction coefficient shows that model also can capture the vertical distribution and the evolution of aerosol extinction coefficient during the fog-haze period (10–15 January)."</p>
Page 18 Line 10~13	Insert "(10–15 January) with the simulated maximum surface PM <sub>2.5</sub> concentration of ~600 ug m <sup>-3</sup> , minimum atmospheric visibility of ~0.3 km and 10–100 hours of simulated hourly surface PM <sub>2.5</sub> concentration above 300 ug m <sup>-3</sup> over NCP "
Page 18 Line 19	Change "radiation" to "energy flux"
Page 23 Line 6~7	Insert "For the average differences between Beijing, Tianjin and Hebei, "

<p>Page 25 Line 22~ Page 26 Line 14</p>	<p>Insert "There are uncertainties in this study. The model overestimates PM2.5 at Xianghe and Tianjin according to Figure 3. The diurnal variation of PM2.5 at Xianghe and Tianjin from model results and observations shows that the overestimation is basically at night which may relate to the setting of atmospheric boundary layer height at night in the model and also the bias of emission inputted to the model. As the aerosol feedback derived from the aerosol radiative effect mainly has large impacts during daytime, it is noted that the overestimation of PM2.5 may lead to slight overestimation of the aerosol feedback during the pollutant period. Emission with higher resolution may be useful for improving the model performance. The aerosol direct and indirect effect is also very sensitive to the mixing state between scattering aerosols and absorbing aerosols. Moreover, the feedback between aerosol and cloud/meteorological parameters also has large uncertainty. Although aerosol indirect forcing is considered in WRF-Chem, it only includes the aerosol effect on resolved stratiform clouds. With a horizontal resolution of 27 km, convective clouds are still parameterized in the model without explicit cloud microphysics in the convective cloud parameterization that links aerosols to cloud condensation or ice nuclei."</p>
<p>Page 26 Line 18~23</p>	<p>Change "This work was supported by the National Basic Research Program of China (2014CB953802), the "Strategic Priority Research Program (B)" of the Chinese Academy of Sciences (XDB05030105, XDB05030102, XDB05030103), and an NSFC project (41305010)." to " This work was supported by the National Basic Research Program of China (2014CB953802), the "Strategic Priority Research Program (B)" of the Chinese Academy of Sciences (XDB05030105, XDB05030102, XDB05030103), the International S&amp;T Cooperation</p>

	Program of China (2011DFG23450), the National Natural Science Foundation of China (41305010) and the Russian Scientific Fund under grant 14-47-00049."
Page 27 Line 27~30	Insert "Che, H., Zhang, X., Chen, H., Damiri, B., Goloub, P., Li, Z., Zhang, X., Wei, Y., Zhou, H., Dong, F., Li, D., and Zhou, T.: Instrument calibration and aerosol optical depth validation of the China Aerosol Remote Sensing Network, <i>J. Geophys. Res.</i> , 114, D03206, doi:10.1029/2008JD011030, 2009a."
Page 28 Line 4	Change "2009" to "2009b"
Page 29 Line 16~18	Insert "He, K. B.: Multi-resolution Emission Inventory for China (MEIC): model framework and 1990-2010 anthropogenic emissions, International Global Atmospheric Chemistry Conference, 17-21 September, Beijing, China, 2012."
Page 29 Line 32~34	Insert "Lei, Y., Zhang, Q., He, K.B., and Streets, D.G.: Primary anthropogenic aerosol emission trends for China, 1990–2005, <i>Atmos. Chem. Phys.</i> , 11, 931–954 <a href="http://dx.doi.org/10.5194/acp-11-931-2011">http://dx.doi.org/10.5194/acp-11-931-2011</a> , 2011."
Page 33 Table 1	Revised
Page 35 Figure 1	Revised
Page 35 caption of Figure 1	Change to "Figure 1. Study domain and regional divisions: Hebei Province, Beijing, Tianjin, Inner Mongolia, Shanxi Province, and Shandong province. The observation sites (BJ, MY, BD, TS, TJ, QHD and SJZ) from CNMC are denoted as circles and those from the CARE-China network (BJ, TJ, XH and XL) are denoted as stars, of which BJ and TJ from CNMC and the CARE-China network are very close. The observation sites (BJ, XL and XH) from AERONET have the same locations as those from CARE-China. Huimin site from Che et al. (2014) is denoted as a cross. The

	black box denotes the region of Beijing, Tianjin and Hebei Province (BTH region, 36.2°–41°N, 114°–118°E), and the three blue boxes with dashed lines denote Beijing, Tianjin and south Hebei Province, respectively."
Page 41 Figure 5	Revised
Page 41 caption of Figure 5	Change to "Figure 5. Time series of daily AOD at 550 nm from AERONET measurements at BJ, XL and XH site and from Che et al. (2014) at Huimin site (daily average) and MODIS retrievals (at 13:00 local time) and the corresponding WRF-Chem simulation (EXP_CTL) for daily average (solid black line) and at 13:00 local time (dash black line) during 2–26 January 2013."
Page 42 Line 4 caption of Figure 6	Change "radiation" to "energy flux"

1 |  
2 **Modeling the feedback between aerosol and**  
3 **meteorological variables in the atmospheric boundary**  
4 **layer during a severe fog-haze event over the North**  
5 **China Plain**

6  
7 Yi Gao<sup>1</sup>, Meigen Zhang<sup>\*1</sup>, Zirui Liu<sup>1</sup>, Lili Wang<sup>1</sup>, Pucai Wang<sup>2</sup>, Xiangao  
8 Xia<sup>2</sup>, and Minghui Tao<sup>3</sup>

9  
10 *<sup>1</sup>State Key Laboratory of Atmospheric Boundary Layer Physics and Atmospheric*  
11 *Chemistry (LAPC), Institute of Atmospheric Physics, Chinese Academy of Sciences,*  
12 *Beijing, China*

13 *<sup>2</sup>Key Laboratory of Middle Atmosphere and Global Environment Observation (LAGEO),*  
14 *Institute of Atmospheric Physics, Chinese Academy of Sciences, Beijing, China*

15 *<sup>3</sup>State Key Laboratory of Remote Sensing Science, Institute of Remote Sensing and*  
16 *Digital Earth, Chinese Academy of Sciences, Beijing, China*

17  
18  
19  
20  
21  
22  
23  
24  
25  
26 \*Corresponding author:

27  
28 Meigen Zhang

29 State Key Laboratory of Atmospheric Boundary Layer Physics and Atmospheric  
30 Chemistry (LAPC)

31 Institute of Atmospheric Physics

32 Chinese Academy of Sciences

33 Huayanli 40#, Chaoyang District, Beijing, China, 100029

34  
35 Tel: 010-62040159(o)

36 E-mail: [mgzhang@mail.iap.ac.cn](mailto:mgzhang@mail.iap.ac.cn)

37  
38  
39

1 **Abstract**

2 The feedback between aerosol and meteorological variables in the atmospheric  
3 boundary layer over the North China Plain (NCP) is analyzed by conducting numerical  
4 experiments with and without the aerosol direct and indirect effects via a coupled  
5 meteorology and aerosol/chemistry model (WRF-Chem). The numerical experiments are  
6 performed for the period 2–26 January 2013, during which a severe fog-haze event (10–  
7 15 January 2013) occurred with the simulated maximum hourly surface PM<sub>2.5</sub>  
8 concentration of ~600 ug m<sup>-3</sup>, minimum atmospheric visibility of ~0.3 km and 10–100  
9 hours of simulated hourly surface PM<sub>2.5</sub> concentration above 300 ug m<sup>-3</sup> over NCP.  
10 Comparison of ~~the~~ model results with aerosol feedback against observations indicates  
11 that the model can reproduce the spatial and temporal characteristics of temperature,  
12 relative humidity (RH), wind, surface PM<sub>2.5</sub> concentration, atmospheric visibility, and  
13 aerosol optical depth reasonably well. ~~Comparison-Analysis~~ of modeling results ~~in the~~  
14 ~~presence and absence of~~ with and without aerosol feedback shows that during the fog-  
15 haze event ~~shows that~~ aerosols lead to a significant negative radiative forcing of -20–140  
16 W m<sup>-2</sup> at the surface and a large positive radiative forcing of 20–120 W m<sup>-2</sup> in the  
17 atmosphere and induce significant changes in meteorological variables ~~of which they~~ with  
18 maximum changes ~~occur~~ during 09:00-18:00 (LT) over urban Beijing and Tianjin, and  
19 south Hebei Province: the temperature decreases by 0.8–2.8 °C at the surface and  
20 increases by 0.1–0.5 °C at around 925 hPa while the RH increases by about 4–12% at the  
21 surface and decreases by 1–6% at around 925 hPa. As a result, the aerosol-induced  
22 equivalent potential temperature profile change shows that the atmosphere is much more  
23 stable and thus the surface wind speed decreases by up to 0.3 m s<sup>-1</sup> (10%) and the

1 atmosphere boundary layer height decreases by 40–200 m (5–30%) during the daytime of  
2 this severe fog-haze event. Owing to this more stable atmosphere, during 09:00–18:00,  
3 10–15 January, compared to the surface PM<sub>2.5</sub> concentration from the model results  
4 without aerosol feedback, the average surface PM<sub>2.5</sub> concentration increases by 10–50 µg  
5 m<sup>-3</sup> (2–30%) over Beijing, Tianjin, and south Hebei province and the maximum increase  
6 of hourly surface PM<sub>2.5</sub> concentration is around 50 µg m<sup>-3</sup> (70%), 90 µg m<sup>-3</sup> (60%) and  
7 80 µg m<sup>-3</sup> (40%), averaged over Beijing, Tianjin and south Hebei Province, respectively.  
8 Although the aerosol concentration is maximum at nighttime, the mechanism of feedback  
9 by which meteorological variables increase the aerosol concentration most occurs during  
10 the daytime (around 10:00 and 16:00). The results suggest that aerosol induces a more  
11 stable atmosphere, which is favorable for the accumulation of air pollutants, and thus  
12 contributes to the formation of fog-haze events.

13

14

15

16

17

18

19

20

21

22

23

## 1 **1. Introduction**

2 The occurrence of fog-haze events has been more frequent in recent years in the  
3 developing regions and mega-cities of China. These regions, as determined by visibility  
4 observations from the China Meteorological Administration (CMA) (Che et al., 2007,  
5 2009b; Zhang et al., 2012), include: the North China Plain (NCP: Beijing, Tianjin, Hebei  
6 Province, Shanxi Province, and part of Inner Mongolia Province) and Guanzhong Plain,  
7 East China – mainly the Yangtze River Delta area, South China – mostly in the areas of  
8 Guangdong and the Pearl River Delta, and the Sichuan Basin in Southwest China. The  
9 North China Plain (NCP) is one of China’s most important social and economic regions;  
10 it has a huge population and undergone rapid development during recent decades. Large  
11 emission sources emit primary aerosols and the precursors of secondary aerosols (Zhang  
12 et al., 2009; Street et al., 2003), resulting in high loads of aerosols and many aerosol  
13 species [e.g. sulfate ( $\text{SO}_4^{2-}$ ), nitrate ( $\text{NO}_3^-$ ), ammonium ( $\text{NH}_4^+$ ), black carbon (BC),  
14 organic carbon (OC), and dust] over the NCP. This is the main reason for the  
15 deterioration of visibility and fog-haze events through light extinction (Sun et al., 2006;  
16 Chan and Yao, 2008). Based on observational studies (Cheng et al., 2011; Zhao et al.,  
17 2013, Quan et al., 2011), during haze periods, the concentration of particulate matter is  
18 much higher than on normal days, and fine-mode aerosol is predominant on haze days.  
19 Using the RAMS (Regional Atmospheric Modeling System) – CMAQ (Community  
20 Multi-scale Air Quality) modeling system (RAMS–CMAQ), Han et al. (2013) showed  
21 that the low visibility in December 2010 over the NCP was primarily caused by a high  
22 mass burden of  $\text{PM}_{2.5}$  as a result of local pollutant accumulation, long-range transport,

1 and  $\text{SO}_4^{2-}$  and  $\text{NO}_3^-$ , which are the two major inorganic aerosol components of  $\text{PM}_{2.5}$ ,  
2 decreasing visibility by contributing 40% to 45% of the total extinction coefficient value.

3 During ~~11~~10–14–15 January 2013, extremely severe fog-haze occurred over the NCP,  
4 especially over Beijing, Tianjin, and south of Hebei Province with very high aerosol  
5 concentration and extremely low atmospheric visibility. The  $\text{PM}_{2.5}$  (particulate matter of  
6  $2.5\mu\text{m}$  or less in aerodynamic diameter) concentration at Beijing were  $300\text{--}800\ \mu\text{g m}^{-3}$   
7 and the air quality index (AQI) was  $>300$  (AQI above 300 is considered hazardous to all  
8 humans), according to data provided by the Ministry of Environmental Protection (MEP)  
9 of China. This month has been reported as the haziest month of the past 60 years in  
10 Beijing, and the reason for its formation draws much attention and is the focus of many  
11 studies (e.g. H. Wang et al., 2014; Y. S. Wang et al., 2014; Sun et al., 2014; Zhang et al.,  
12 2014; Che et al., 2014; Tao et al., 2014). By analyzing observations from the Campaign  
13 on the Atmospheric Aerosol Research Network of China (CARE-China), Y. S. Wang et  
14 al. (2014) showed that during 9–15 January 2013, the hourly surface  $\text{PM}_{2.5}$  concentration  
15 reached  $680\ \mu\text{g m}^{-3}$  in Beijing, Shijiazhuang (the capital city of Hebei Province), and  
16 Tianjin. It was indicated that a ~~weak weather system~~synoptic scale stagnation, unusually  
17 cold air, and local metrological conditions (which were extremely unfavorable for the  
18 diffusion of air pollutants) were the external reasons, while the rapid transfer from  
19 aerosol precursor to aerosol was the main internal reason, for this fog-haze event (Y. S.  
20 Wang et al., 2014). Sun et al. (2014) showed that the  $\text{PM}_1$  mass concentration during 10–  
21 14 January in Beijing ranged from  $144\text{--}300\ \mu\text{g m}^{-3}$ , which was 10 times higher than that  
22 during clean periods. They also concluded that stagnant meteorological conditions, coal

1 combustion, secondary production, and regional transport were the four main factors  
2 driving the formation and evolution of haze pollution in Beijing during wintertime.

3 It is known that atmospheric aerosols enhance the absorption and scattering of  
4 radiation (direct effect, DE) and act as cloud condensation and ice nuclei that alter cloud  
5 properties and precipitation (indirect effect, IE) (Twomey, 1974; Albrecht, 1989). These  
6 in turn lead to large decreases in solar radiation reaching the earth's surface, increases in  
7 solar heating of the atmosphere, and changes in the distribution of atmospheric  
8 temperature structure and precipitation (Ramanathan et al., 2001). It was shown that  
9 aerosol DE at the surface was  $32.8 \text{ W m}^{-2}$  at Xianghe, a suburban site in the NCP, which  
10 was comparable to that of cloud radiative effect (Li et al., 2007; Xia et al., 2007).  
11 Analysis of a heavy pollution episode in fall of 2004 over northern China showed that the  
12 instantaneous aerosol DE at the surface reached  $350 \text{ W m}^{-2}$  and  $300 \text{ W m}^{-2}$  of which was  
13 absorbed by the atmosphere, therefore, a more stable atmosphere was expected (Liu et al.,  
14 2007). Many modeling studies have indicated a decrease in the seasonal/annual average  
15 temperature at the surface induced by aerosol over China (Qian et al., 2003; Liu et al.,  
16 2010; Wu and Han, 2011; Huang et al., 2006). Wu et al. (2009) used the CAM  
17 (Community Atmosphere Model) to simulate the DE of aerosol ( $\text{SO}_4^{2-}$ , dust, BC, and OC)  
18 on temperature during 1960–2000 and showed that the surface temperature decreased by  
19 about 1.5 K, while atmospheric temperature decreased under 850 hPa and increased in  
20 the middle troposphere.

21 Most of the aforementioned studies focused only on the impacts of meteorological  
22 condition on air quality or aerosol-induced meteorological condition changes on climate  
23 scale, ignoring the feedback from aerosol-induced meteorological conditions change to

1 aerosol concentration and the change of meteorological variables over shorter time scales  
2 (e.g. the diurnal cycle). These may affect the evolution of air pollution, which usually  
3 operates over such shorter time scales. In this paper, we estimate the feedback between  
4 aerosols and meteorological variables in the atmospheric boundary layer over the NCP  
5 during the fog-haze event of 10–15 January 2013 by conducting numerical simulations  
6 using a coupled meteorology and aerosol/chemistry model (WRF-Chem). We begin by  
7 introducing the Weather Research and Forecasting-Chemistry model (WRF-Chem), the  
8 handling of emissions and the numerical experiments in section 2, followed by a  
9 description of the observation data in section 3. Next, we present the model results in  
10 section 4: the performance of WRF-Chem in simulating the meteorological variables,  
11 surface PM<sub>2.5</sub> concentrations, visibility, and aerosol optical depth (AOD) over the NCP;  
12 the aerosol impacts on temperature, relative humidity (RH), energy budget, the equivalent  
13 potential temperature (EPT) profile, wind, and atmospheric (planetary) boundary layer  
14 height (PBLH) during the fog-haze event over the NCP; and the feedback of the above  
15 meteorological variables changes to aerosol concentrations. Finally, a summary of the  
16 key findings is given in section 5.

17

## 18 **2. Model description**

### 19 *2.1 WRF-Chem Model*

20 WRF-Chem is a version of the Weather Research and Forecasting (WRF) model  
21 (Skamarocket al., 2008) that simulates trace gases and aerosol simultaneously with the  
22 meteorological fields (Grell et al., 2005). The version used in this study is based on  
23 v3.2.1, but with updates including the GOCART (Georgia Tech/Goddard Global Ozone

1 Chemistry Aerosol Radiation and Transport) dust emission coupled with  
2 ~~MADE/SORGAM (Modal Aerosol Dynamics Model for Europe and Secondary Organic~~  
3 ~~Aerosol Model) and~~ MOSAIC (Model for Simulating Aerosol Interactions and Chemistry)  
4 (Zhao et al., 2010), and representation of aerosol direct radiative feedback in the Rapid  
5 Radiative Transfer Model for GCMs (RRTMG) radiation (Zhao et al., 2011), which were  
6 released in v3.3. All major components of aerosol are treated in the model, including  
7  $\text{SO}_4^{2-}$ ,  $\text{NO}_3^-$ ,  $\text{NH}_4^+$ , BC, OC, sea salt, mineral dust, and aerosol water. Different aerosol  
8 species are internally mixed within the mode and externally mixed among different  
9 modes. The aerosol scheme includes the representation of physical and chemical  
10 processes of emission, nucleation, condensation, coagulation, aqueous-phase chemistry,  
11 water uptake by aerosols, and dry and wet deposition. Aerosol optical properties such as  
12 extinction, single-scattering albedo, and asymmetry factor for scattering are computed as  
13 a function of wavelength and three-dimensional position. Each chemical constituent of  
14 the aerosol is associated with a complex refraction index calculated by volume averaging  
15 for each size bin (or mode), and Mie theory is used to compute the extinction efficiency  
16 ( $Q_e$ ) and the scattering efficiency ( $Q_s$ ). To efficiently compute  $Q_e$  and  $Q_s$ , WRF-Chem  
17 uses a methodology described by Ghan et al. (2001a) in which the full Mie calculations  
18 are first performed to obtain a table of seven sets of Chebyshev expansion coefficients,  
19 but later are skipped and  $Q_e$  and  $Q_s$  are calculated using bilinear interpolation over the  
20 Chebyshev coefficients stored in the table. A detailed description of the computation of  
21 aerosol optical properties in WRF-Chem can be found in Fast et al. (2006) and Barnard et  
22 al. (2010). Bulk hygroscopicity of each size mode/bin, equivalent to  $k$  in Petters and  
23 Kreidenweis (2007), is based on the volume-weighted average of the hygroscopicity of

1 each aerosol component. The aerosol wet radius is calculated based on Kohler theory.  
2 Aerosol–cloud interactions for the aerosol first and second IEs are included in the model  
3 by Gustufson et al. (2007) for calculating the activation and resuspension between  
4 interstitial aerosols and cloud droplets, which is similar to the method used in the  
5 MIRAGE (Model for Integrated Research on Atmospheric Global Exchanges) general  
6 circulation model (Ghan et al., 2001b). Aerosol activation is parameterized in terms of  
7 updraft velocity and the properties (number, size and hygroscopicity) of all of the aerosol  
8 modes (Abdul-Razzak and Ghan, 2000). The autoconversion of cloud water to rain water  
9 depends on cloud droplet number, following Liu et al. (2005).

## 10 *2.2 Numerical experiments and emissions*

11 In this study, WRF-Chem is configured to cover the east part of China (101 °–134 °E,  
12 25 °–46 °N) with 80 (S–N) ×90 (W–E) grid points at 27 km horizontal resolution centering  
13 on Central China (117 °E, 36 °N), and 51 vertical layers up to 50hPa with 25 layers under  
14 850 hPa. Figure 1 shows the study domain used in this paper. The Morrison two-moment  
15 bulk microphysics scheme is used to include the aerosol IE (Gustafson et al., 2007) and  
16 the RRTMG longwave/shortwave scheme is used to include the aerosol DE (Zhao et al.,  
17 2011). The CBMZ (carbon bond mechanism) and MOSAIC (Model for Simulating  
18 Aerosol Interactions and Chemistry) (Zaveri et al., 2008; Fast et al., 2006) are used in this  
19 study. MOSAIC uses a sectional approach where the aerosol size distribution is divided  
20 into discrete size bins defined by their lower and upper dry particle diameters. In this  
21 study, the aerosol size is divided into eight bins. The initial meteorological fields and  
22 boundary conditions are from the National Centers for Environmental Prediction (NCEP)  
23 Final Reanalysis data. Both the initial and boundary chemical conditions are from

1 | MOAZART's (Model for OZone and Related chemical Tracers) chemical boundary  
2 | conditions which are specific to the period being studied.-

3 |       The simulation is conducted from 14 December 2012 to 26 January 2013, including  
4 | the time for model spin-up. Two numerical experiments are conducted in order to  
5 | investigate the feedback between aerosol and meteorological variables. The baseline  
6 | experiment (EXP\_CTL) is conducted by the WRF-Chem model with standard  
7 | anthropogenic emissions (see section 2.3) and full coupling of aerosol and meteorology  
8 | simulation. The sensitivity experiment (EXP\_NOEF) is conducted by closing the  
9 | feedback between aerosol and meteorological variables, i.e. eliminating the aerosol DE  
10 | and IE in the model. The effect of aerosol on meteorological variables and the feedback  
11 | of the aerosol-induced meteorological variables changes to aerosol concentrations can be  
12 | estimated as the difference between EXP\_CTL and EXP\_NOEF. The model results from  
13 | EXP\_CTL during 2–26 January 2013 are used for the model evaluation, while the  
14 | difference between the numerical experiment results from 10–15 January 2013, the fog-  
15 | haze period, is analyzed to study aerosol feedback effects.

### 16 | *2.3 Emissions*

17 |       Anthropogenic emissions of carbon monoxide (CO), nitrogen oxides (NO<sub>x</sub>), SO<sub>2</sub>,  
18 | volatile organic compounds (VOCs), BC, OC, PM<sub>2.5</sub>, and PM<sub>10</sub> are based on Tsinghua  
19 | University's 2010 monthly emission inventory (Lei et al., 2011, Zhang et al.,  
20 | 2009, and He et al., 2012), and are added to the diurnal information based on Wang et al.  
21 | (2010). We use the 2010 NH<sub>3</sub> emission from the Regional Emission inventory for the  
22 | Asia domain (REAS, <http://www.jamstec.go.jp/frsgc/research/d4/emission.htm>).  
23 | Biomass-burning emission is obtained from the Global Fire Emissions Database, Version

1 3 (GFEDv3) with monthly temporal resolution (Randerson et al., 2005). Biogenic  
2 emission is from the Model of Emission of Gases and Aerosol from Nature (MEGAN)  
3 (Guenther et al., 2006). Dust emission is calculated online following Zhao et al. (2010).  
4 Sea salt emission is calculated online following Gong et al. (1997) in the publically  
5 released version of WRF-Chem. In this study, the sea salt emission scheme is updated  
6 following Gong (2003) to include the correction of particles with radius less than 0.2  $\mu\text{m}$ ,  
7 and Jaeglé et al. (2011) to include the sea salt emission dependence on sea surface  
8 temperature.

9

### 10 **3. Observation data**

11 The monitoring of meteorological data and visibility from the surface stations of the  
12 Chinese National Meteorological Center (CNMC; <http://cdc.cma.gov.cn/home.do>) were  
13 collected to evaluate the performance of the meteorological field simulation. CNMC has  
14 726 measurement stations that are evenly distributed throughout mainland China and has  
15 been providing long-term surface observations of several meteorological variables since 1  
16 January 1951 (Feng et al., 2004). The sites used in the study include: BJ (54511, Beijing,  
17 39.8  $\text{N}$ , 116.47  $\text{E}$ ), MY (54416, Miyun, 40.38  $\text{N}$ , 116.87  $\text{E}$ ), BD (54602, Baoding,  
18 38.85  $\text{N}$ , 115.52  $\text{E}$ ), TS (54534, Tangshan, 39.07  $\text{N}$ , 118.15  $\text{E}$ ), TJ (54527, Tianjin,  
19 39.08  $\text{N}$ , 117.07  $\text{E}$ ), QHD (54449, Qinhuangdao, 39.85  $\text{N}$ , 119.52  $\text{E}$ ), and SJZ (53698,  
20 Shijiazhuang, 38.03  $\text{N}$ , 114.42  $\text{E}$ ). Each site is denoted as a circle in Fig. 1.

21 The surface  $\text{PM}_{2.5}$  concentrations from 2–26 January 2013 are from the CARE-  
22 China network (Y. S. Wang et al., 2014), which is located in the Jing-Jin-Ji area. The  
23 sites include BJ (Beijing, 39.97  $\text{N}$ , 116.37  $\text{E}$ ), XL (Xinglong, 40.39  $\text{N}$ , 117.58  $\text{E}$ ), XH

1 (Xianghe, 39.75 °N, 116.96 °E), and TJ (Tianjin, 39.08 °N, 117.21 °E), of which BJ and TJ  
2 are urban sites, XH is a suburban site, and XL is considered as the background area of the  
3 NCP. Observational sites in the CARE-China network are equipped with RP1400-PM<sub>2.5</sub>  
4 or RP1405-PM<sub>2.5</sub> (ThermoScientific: <http://www.thermoscientific.com>), which provide a  
5 continuous direct mass measurement of particulates by utilizing a tapered element  
6 oscillating microbalance (TEOM) (Patashnick and Rupprecht, 1991). Each site is denoted  
7 as a star in Fig. 1.

8 The Aerosol Robotic Network (AERONET) (Holben et al., 1998) is a network of  
9 sun- and sky-scanning ground-based automated radiometers providing data on aerosol  
10 optical properties (Dubovik and King, 2000; Dubovik et al., 2002). In this study, we use  
11 the Level 2.0 AOD data in 2013. The three sites are BJ [Beijing, 39.98 °N, 116.38 °E, 30  
12 m.s.l.(Mean Surface Level)], XL (Xinglong, 40.39 °N, 117.58 °E, 940 m.s.l.), and XH  
13 (Xianghe, 39.75 °N, 116.99 °E, 80 m.s.l.), which have the same locations as the sites in the  
14 CARE-China network.

15 [AOD data at Huimin site \(37.48 °N, 117.53 °E, 11.7 m.s.l.\) from Che et al. \(2014\)](#)  
16 [which is collected from the China Aerosol Remote Sensing Network \(CARSNET\) and](#)  
17 [were processed using the ASTPwin software offered by Cimel Ltd. Co \(Che et al., 2009a\)](#)  
18 [is also used. This site is denoted as a cross in Fig.1.](#)

19 The Moderate Resolution Imaging Spectroradiometer (MODIS) aboard the Terra  
20 and Aqua satellites covers eastern China twice a day at around 1100 and 1300 local time,  
21 respectively. The Collection 6 MODIS enhanced Deep Blue algorithm provides 10 km  
22 aerosol data over all cloud-free land surfaces except for snow-covered regions with  
23 expected errors within 0.05±20% (Hsu et al., 2013). The improved cloud mask method

1 allows more aerosol retrievals in heavy aerosol loading conditions, making Collection 6  
2 MODIS aerosol data more suitable for monitoring haze pollution in eastern China.

3

#### 4 **4. Results and discussion**

##### 5 *4.1 Model result for meteorological variables, surface $PM_{2.5}$ concentration, visibility, and* 6 *aerosol optical depth*

7 In this section, a comparison between the model results for temperature, RH, wind,  
8 surface  $PM_{2.5}$  concentration, visibility, and AOD from EXP\_CTL and observations  
9 during 2–26 January 2013 is presented. Figure 2 are the time series of observed and  
10 simulated daily-averaged surface temperature, surface RH, precipitation, surface wind  
11 speed, and wind direction at BJ, MY, BD, TS, TJ, and QHD during 2–26 January 2013,  
12 respectively. The corresponding statistical analysis of the comparisons between simulated  
13 and observed temperature, RH, and wind is presented in Table 1. As seen in Fig. 2, the  
14 simulated meteorological variables agree well with observations. For the temperature, the  
15 model can depict its temporal variation but slightly underestimates the values at BJ and  
16 TJ, with correlation coefficients ( $R$ ) of 0.78–0.91 and mean bias ( $MB$ ) of  $-1.6\text{ }^{\circ}\text{C}$  to  $0.5\text{ }^{\circ}\text{C}$   
17 at the six sites. The model also reproduces the spatial distribution of temperature: the  
18 temperature is minimum at MY and QHD, of which MY is at the highest latitude and  
19 QHD is a coastal site (Fig. 1); while the maximum is at BJ and TJ, which are both urban  
20 sites located in big cities. The observed RH is also reasonably reproduced by the model  
21 ( $R = 0.72\text{--}0.90$ ;  $MB = -10.0\%$  to  $-8.8\%$ ). During 10–15 January, both the simulated and  
22 observed RH are very high, with values ranging from 70% to 90%, especially at BD, TS,  
23 TJ, and QHD, which may be influenced by the south and southeast wind flow from more

1 moist areas (Gao et al., 2014). The high RH over the NCP will contribute to the high  
2 aerosol concentration and fog-haze event during 10–15 January (Zhang et al., 2014).  
3 From Fig. 2, the model also reproduces the precipitation during 20–21 January but  
4 underestimates the values of daily precipitation. This may be due to the relatively coarse  
5 model resolution (27 km) that is unable to resolve the local variability at each site. There  
6 is no precipitation during the fog-haze period (10–15 January). The simulated variation of  
7 the maximum and mean wind speed and wind direction in the model agree well with the  
8 observation at the six sites ( $R = 0.51$ – $0.83$  for mean wind speed and  $0.22$ – $0.86$  for wind  
9 direction). However, the model overestimates the mean wind speed by  $0.5$ – $1.9 \text{ m s}^{-1}$  at  
10 the six sites. This may be due to the out-of-date land surface data in the model which is  
11 adopted from 5 min resolution USGS (United States Geological Survey) 24 category data  
12 derived from 1 km Advanced Very High Resolution Radiometer (AVHRR) measurement  
13 in a 12-month period spanning from April 1992 to March 1993 (Loveland et al., 1991;  
14 Brown et al., 1993). The USGS datasets may underestimate the urbanization over NCP  
15 comparing with ~~nowadays~~ present-day land surface data (Yu et al., 2012). The maximum  
16 wind speed is simulated much better by the model than the mean wind speed [ $R = 0.60$ –  
17  $0.76$ , normalized mean bias ( $NMB$ ) =  $6\%$ – $20\%$ ]. The reason may be that the simulated  
18 wind speed is instantaneous while the observed mean wind speed is ten-minutes averaged.  
19 In addition, the out-of-data land surface data make the small wind speed cannot be well  
20 reproduced by model.

21 Figure 3 shows the time series of hourly surface  $\text{PM}_{2.5}$  concentration from the  
22 observation and the corresponding model results from EXP\_CTL at BJ, XL, XH, and TJ  
23 during 2–26 January 2013. The statistical analysis between the model results and

1 observation of surface  $PM_{2.5}$  concentration is shown in Table 1. In general, the model  
2 reasonably reproduces the hourly variation of surface  $PM_{2.5}$  concentration during 2–26  
3 January at the four sites ( $R = 0.56–0.69$ ,  $NMB = -10.9\%–59.5\%$ ). Both the observation  
4 and model results show the surface  $PM_{2.5}$  concentration to be highest at XH and TJ, of  
5 which XH is a suburban site located in Hebei Province and TJ is an urban site located in  
6 Tianjin. Note that although XH is a suburban site, the surface  $PM_{2.5}$  concentration at this  
7 site is comparable to, or even higher than, that at BJ (Fig. 3 and Table 1), which may  
8 suggest more pollutants over the south part of Hebei Province and transport of pollution  
9 to Beijing. The surface  $PM_{2.5}$  concentration is lowest at XL, which is a background site  
10 located at the top of a mountain (940 m.s.l.) and less affected by anthropogenic activities  
11 and more affected by transport compared to other sites. The simulated surface  $PM_{2.5}$   
12 concentration agrees very well with the observation at XL ( $R = 0.69$ ), indicating that the  
13 atmospheric transport process is reproduced by the model. The model overestimates the  
14 surface  $PM_{2.5}$  concentration at XH and TJ. In Fig. 3, focusing on the fog-haze period (10–  
15 15 January), it can be seen that the event starts from midnight on 10 January, with the  
16 surface  $PM_{2.5}$  concentration rising from around 100 to 200–300  $\mu\text{g m}^{-3}$  at BJ, from  
17 around 50 to 200–300  $\mu\text{g m}^{-3}$  at XL, and from 100 to 200–400  $\mu\text{g m}^{-3}$  at XH and TJ.  
18 After that, the concentration continues to increase to 200–400  $\mu\text{g m}^{-3}$  at BJ and XL, and  
19 to 300–500  $\mu\text{g m}^{-3}$  at XH and TJ, during the daytime of 11 January. The surface  $PM_{2.5}$   
20 concentration decreases during the night on 11 January at BJ and XL, but maintains a  
21 high value of 200–500  $\mu\text{g m}^{-3}$  at XH and TJ. The surface concentration increases again  
22 on 12 and 13 January, with a value of 200–400  $\mu\text{g m}^{-3}$  at BJ, 100–200  $\mu\text{g m}^{-3}$  at XL, and  
23 200–500  $\mu\text{g m}^{-3}$  at XL and TJ. During the nighttime of 14 January, the surface  $PM_{2.5}$

1 concentration begins to decrease to around 50–100  $\mu\text{g m}^{-3}$  at all four sites. The consistent  
2 variation of surface  $\text{PM}_{2.5}$  concentration at the four sites and the rapid rise of surface  
3  $\text{PM}_{2.5}$  concentration at XL suggest that the fog-haze event of 10–15 January 2013 was  
4 regionally distributed.

5 Figure 4 is the time series of hourly visibility at 00:00, 06:00, 12:00 and 18:00 from  
6 CNMC measurements and the corresponding WRF-Chem simulation at BJ, TJ, BD, and  
7 SJZ during 2–26 January 2013. The visibility is calculated as  $3.912/\text{aerosol extinction}$   
8 coefficient at 550nm. The impacts of gas phase molecules on visibility include Rayleigh  
9 scattering of air, and the absorptions of  $\text{O}_3$ ,  $\text{NO}_2$ , and  $\text{SO}_2$  of solar radiation are small  
10 compared with the droplets and particles under heavy aerosol loading conditions. As a  
11 result, their effects on visibility are ignored in this study (Deng et al., 2008; Quan et al.,  
12 2011). The simulated aerosol extinction coefficient at 550nm is calculated by using the  
13 default output AOD and Angstrom exponent derived from the output AODs at 400nm  
14 and 600nm. Therefore, the evaluation of the modeled visibility also reflects the  
15 evaluation of the modeled aerosol concentration and optical properties. From Fig. 4 and  
16 Table 1, the visibility is reproduced well by the model ( $R = 0.77, 0.66, 0.58,$  and  $0.43$  and  
17  $\text{MB} = 5.0, 0.1, 0.7,$  and  $-0.2$  km at the four sites, respectively). The model overestimates  
18 the visibility at BJ, and the overestimation is mainly due to the overestimation of  
19 visibility on clear days. This may be caused by the bias of the modeled extinction  
20 coefficient and aerosol mass concentration. Nevertheless, the model is able to capture the  
21 deterioration of visibility on polluted days at the four sites. Both the observation and  
22 model results show the value of visibility to be very low (around 1–3 km) during 10–14

1 January. However, the model overestimates the visibility at BJ on 12 January, which may  
2 be due to the underestimated surface PM<sub>2.5</sub> concentration on 12 January (Fig. 3).

3 Figure 5 is the time series of daily AOD at 550 nm from the AERONET  
4 measurements at BJ, XL, and XH and Che et al. (2014) at Huimin site and MODIS deep-  
5 blue AOD retrievals and the corresponding WRF-Chem simulation ~~at BJ, XL, and XH~~  
6 during 2–26 January 2013. The simulated AOD at 550nm is calculated by using the  
7 Angstrom exponent derived from the default output AODs at 400nm and 600nm. As the  
8 MODIS aboard the Aqua satellites covers eastern China at around 13:00 local time, the  
9 simulated AOD at 13:00 is showed in Figure 5. Statistical analysis of the comparison  
10 between the simulated and observed daily AOD from AERONET is presented in Table 1.  
11 As seen in Fig. 5, the model also reasonably reproduces the day-to-day variations of the  
12 observed AOD by AERONET and MODIS, although there are several missing data; the  
13 R values between the simulated and observed AODs from AERONET are 0.59, 0.99, ~~and~~  
14 0.60 and 0.74 for the BJ, XL, ~~and~~ XH and Huimin sites, respectively. The AOD from  
15 MODIS is much higher than that from AERONET, indicating that the AOD may be  
16 overestimated by MODIS. The modeled averaged AOD is ~~highest-higher~~ at XH and  
17 ~~lowest-lower~~ at XL, consistent with the surface PM<sub>2.5</sub> concentration at these two sites  
18 (Fig. 3). Although model underestimates AOD at Huimin site with the MB of -0.22, both  
19 observation and model result show that the AOD at Huimin site is highest among the four  
20 sites. Considering the location of Huimin site in Figure 1, this indicates that model can  
21 reproduce the more serious pollution to the south of Beijing province.

22 In addition, in the supplement file, the comparison of AOD from MODIS  
23 observations and the corresponding model results shows that model can reproduce the

1 more pollutants over the south part of Hebei Province and the evolution of AOD values;  
2 the comparison of aerosol extinction coefficient from Cloud-Aerosol Lidar and Infrared  
3 Pathfinder Satellite Observations (CALIPSO) and the modeled aerosol extinction  
4 coefficient shows that model also can capture the vertical distribution and the evolution  
5 of aerosol extinction coefficient during the fog-haze period (10–15 January).

#### 7 *4.2 Aerosol impacts on surface energy, meteorological variables, and atmospheric* 8 *stability*

9 In this section, the aerosol radiative forcing (ARF) and its impacts on surface energy,  
10 temperature, RH, atmospheric stability, wind, and PBLH during the fog-haze period (10–  
11 15 January) with the simulated maximum surface PM<sub>2.5</sub> concentration of ~600 ug m<sup>-3</sup>,  
12 minimum atmospheric visibility of ~0.3 km and 10–100 hours of simulated hourly  
13 surface PM<sub>2.5</sub> concentration above 300 ug m<sup>-3</sup> over NCP are presented. Beijing, Tianjin,  
14 and south Hebei Province [BTH region, (36.2 °–41 °N, 114 °–118 °E), black box in Fig. 1]  
15 is the key high-aerosol-concentration region over the NCP where there may be significant  
16 impacts of aerosol on meteorological variables in the atmospheric boundary layer. Figure  
17 6 is the time series of aerosol-induced daily and diurnal change in the surface energy  
18 budget [latent heat (LH), sensible heat (SH), shortwave (SW) radiation, longwave (LW)  
19 radiation, and net ~~radiation~~ energy flux (LH+LW+SH+SW)] and meteorological  
20 variables (temperature at 2m, RH at 2m) averaged for the BTH region, which is  
21 calculated by subtracting the model results of EXP\_NOEF from those of EXP\_CTL. The  
22 diurnal change is calculated for 10–15 January, the pollution episode. Positive values  
23 indicate more energy flux toward the surface, or reduced energy flux away from the

1 surface. Figure 6a shows that during 2–26 January, the SW fluxes at the surface are  
2 reduced by 8–36  $\text{W m}^{-2}$  due to aerosol scattering and absorption of solar radiation at the  
3 surface. The SW fluxes are reduced by 25–35  $\text{W m}^{-2}$  during 10–15 January. The LW  
4 fluxes are increased slightly by up to 6  $\text{W m}^{-2}$  during 2–26 January, with values of 4–6  
5  $\text{W m}^{-2}$  during 10–15 January, due to the positive radiative forcing in the atmospheric by  
6 aerosol. Because of the cooling effect of aerosol at the surface, the LH and SH fluxes  
7 from the surface to the atmosphere during 2–26 January are also reduced by 1–5  $\text{W m}^{-2}$   
8 and 5–16  $\text{W m}^{-2}$ , respectively. The net energy fluxes at the surface are reduced by 15–50  
9  $\text{W m}^{-2}$ , with values of 39–47  $\text{W m}^{-2}$  during 10–15 January. Therefore, during the fog-  
10 haze period, the energy arriving at the surface was largely reduced. In Fig. 6c, the diurnal  
11 change shows the change of surface energy is significant during the daytime: during 10–  
12 15 January, at 09:00–18:00, aerosol reduces SW fluxes, LH fluxes, and SH fluxes by 10–  
13 105, 2–16, and 9–46  $\text{W m}^{-2}$  respectively, and increases LW fluxes by 2–10  $\text{W m}^{-2}$ ; while  
14 during the nighttime, aerosol only increases the LW flux from the atmosphere to the  
15 surface by  $\sim 3 \text{ W m}^{-2}$ . The net surface energy decreases by 6–156  $\text{W m}^{-2}$  during 09:00–  
16 18:00 and increases by a slightly positive value of around  $\sim 1.5 \text{ W m}^{-2}$  during 00:00–  
17 07:00 and 18:00–23:00, which may lead to surface cooling during the daytime.

18 For the daily variation of aerosol-induced 2m temperature and 2m RH, in Fig. 6b,  
19 averaged for the BTH region, aerosols induce a reduction of surface temperature by 0.2–  
20 1.3  $^{\circ}\text{C}$  during 2–26 January, with values of 0.8–1.3  $^{\circ}\text{C}$  during 10–15 January, the largest  
21 reduction during 2–26 January. Aerosols slightly lead to an increase of the surface RH by  
22 0.5–4% during 2–26 January. For the diurnal change depicted in Fig. 6d, it can be seen  
23 that the reduction of surface temperature is at a maximum of 0.7–1.1  $^{\circ}\text{C}$  during 09:00–

1 18:00, but remains at around 0.6 °C during 00:00–08:00 and 19:00–23:00. The aerosol-  
2 induced surface RH increases by 2–5% during 09:00–18:00, but by only 1–2% during  
3 00:00–08:00 and 19:00–23:00. In general, the changes in meteorological variables take  
4 place mainly during the daytime (09:00–18:00).

5 Figure 7 is the spatial distribution of ARF at the bottom of the atmosphere and in the  
6 atmosphere and the aerosol impacts on 2m temperature and 2m RH, calculated by  
7 subtracting the model results of EXP\_NOEF from those of EXP\_CTL averaged during  
8 09:00–18:00, 10–15 January. From Fig. 7a, the ARF at the bottom is highest over south  
9 Hebei Province and Tianjin, with values of  $-80$  to  $-140$   $\text{W m}^{-2}$ , and ranges from  $-60$  to  
10  $-100$   $\text{W m}^{-2}$  over south Beijing. Che et al. (2014) analyzed observations at several sites  
11 over the NCP during January 2013 and indicated that the daily ARF during 10–15  
12 January at the surface was about  $-50$  to  $-75$   $\text{W m}^{-2}$  over north Beijing, and about  $-100$  to  
13  $-150$   $\text{W m}^{-2}$  over south Beijing and Hebei Province. These results are to some extent  
14 consistent with the model results in Fig. 7a. Contrary to the significant negative ARF at  
15 the bottom, the ARF in the atmosphere in Fig. 7b shows that there is a large positive ARF  
16 with the value of  $40$  to  $120$   $\text{W m}^{-2}$  over south Hebei Province and Tianjin, and  $20$  to  $80$   
17  $\text{W m}^{-2}$  over south Beijing. Therefore, a more stable atmosphere is expected. In Fig. 7c,  
18 the aerosol-induced surface temperature decreases most over Tianjin and south Hebei  
19 Province, with values of  $-1.6$  to  $-2.8$  °C. The temperature also decreases by about  $0.4$  to  
20  $1.6$  °C over Beijing and other parts of Hebei Province. Such a reduction of temperature is  
21 a reflection of the decrease in solar radiation reaching the earth's surface due to aerosols.  
22 In Fig. 7c, the aerosol-induced surface RH increases by about 8–14% over south Hebei  
23 Province, by 4–6% over Tianjin, and by 2–4% over Beijing. As the aerosol-induced

1 change in water vapor mixing ratio is very small (1–2%) over the NCP area (figure not  
2 shown), the decrease in temperature can lead to a decrease in the saturation pressure of  
3 water vapor and an increase in RH at the surface, which is beneficial for the hygroscopic  
4 growth of aerosols. Figure 8 is the time–altitude distribution of the diurnal cycle of  
5 aerosol impacts on temperature and RH averaged for the BTH region during 10–15  
6 January. In Fig. 8a it can be seen that, consistent with Fig. 7a, the temperature decreases  
7 near the surface (under 950hPa), with the highest reduction (0.5–1.5 °C) during 09:00–  
8 18:00, while it increases by 0.1–0.5 °C between 950 hPa and 850 hPa during 11:00–16:00.  
9 Such a change in temperature can increase the stability of the atmosphere during daytime.  
10 For RH (Fig. 8b), similar to the change at the surface, its change is opposite to the change  
11 in temperature, increasing by about 2–4% under 950 hPa and decreasing by about 1–6%  
12 between 950 hPa and 850 hPa during 09:00–20:00.

13 From the above discussion, the aerosol-induced change of the solar radiation and  
14 meteorological variables may change the stability of the atmosphere during the fog-haze  
15 event. The profile of the equivalent potential temperature (EPT) can be used to  
16 characterize the stability of the atmosphere. Figure 9 is the aerosol impact on EPT  
17 profiles at 00:00, 06:00, 12:00, and 18:00, averaged during 10–15 January in the BTH  
18 region. As seen in Fig. 9, the impact of aerosol on EPT does not change too much with  
19 altitude at 00:00 and 06:00: the EPT decreases by up to around 0.7 K under 950 hPa. At  
20 12:00, aerosol decreases the EPT near the surface (under 925 hPa) by up to around 1.3 K,  
21 and increases it between 925 hPa and 750 hPa by up to 0.12 K. This suggests that, at  
22 12:00, aerosol leads to a more stable atmosphere. Aerosol decreases EPT by up to around  
23 1.1 K under 875 hPa at 18:00.

1 As a results of the more stable atmosphere, Fig. 10 shows the diurnal variation of  
2 surface  $\text{PM}_{2.5}$  concentration from EXP\_CTL and aerosol-induced 10m wind speed and  
3 PBLH change. In Fig. 10, averaged for the BTH region, the aerosol-induced surface wind  
4 speed decreases during 09:00–18:00, with values of  $0.1\text{--}0.34 \text{ m s}^{-1}$  (3–10%), while there  
5 is no change at other times of the night. The maximum decrease of wind speed is during  
6 14:00–16:00. The decrease of surface wind speed is not favorable for the diffusion of air  
7 pollutants. The PBLH decreases by  $22\text{--}207 \text{ m}$  (8–32%) during 09:00–17:00, with the  
8 maximum reduction (17–32%) seen during 13:00–16:00. The large decrease of PBLH is  
9 beneficial for the accumulation of the air pollutant. It is noticed that the surface  $\text{PM}_{2.5}$   
10 concentration is lowest during 11:00–16:00. This indicates that the changed  
11 meteorological condition will have the largest impacts on the lowest  $\text{PM}_{2.5}$  concentration.

#### 12 *4.3 Feedback of aerosol-induced meteorological variables changes to aerosol* 13 *concentration*

14 The above changes in meteorological variables as a result of aerosol effects (e.g. the  
15 decrease of temperature at the surface and the increase of temperature in the middle  
16 atmosphere, the increase of RH at the surface and in the lower atmosphere, the more  
17 stable atmosphere and the decrease in wind speed and PBLH) can have impacts on the  
18 surface  $\text{PM}_{2.5}$  concentration and eventually contribute to the maintenance and  
19 deterioration of regional air pollution. Figures 11a, c, and e show the hourly surface  
20  $\text{PM}_{2.5}$  concentration from EXP\_NOEF and the impacts of changes in meteorological  
21 variables on hourly surface  $\text{PM}_{2.5}$  concentration averaged for the three sub-regions of the  
22 BTH (Beijing, Tianjin and Hebei, three boxes with blue dash lines in Fig. 1) during 2–26  
23 January. The corresponding diurnal change during 10–15 January are shown in Fig. 11b,

1 d, and f. The change in percentage is calculated by comparing with the surface  $\text{PM}_{2.5}$   
2 concentration from EXP\_NOEF. Among the three sub-regions of the BTH, surface  $\text{PM}_{2.5}$   
3 concentration is highest over Hebei. It can be seen that the maximum increase of  
4 meteorological-variables-change-induced surface  $\text{PM}_{2.5}$  concentration is around  $50 \mu\text{g}$   
5  $\text{m}^{-3}$  (70%),  $90 \mu\text{g m}^{-3}$  (60%), and  $80 \mu\text{g m}^{-3}$  (40%) for Beijing, Tianjin, and Hebei,  
6 respectively, during 10–15 January. For the average differences between Beijing, Tianjin  
7 and Hebei, tThe higher the surface  $\text{PM}_{2.5}$  concentration is, the greater the increase is in  
8 the surface  $\text{PM}_{2.5}$  concentration produced by unfavorable meteorological conditions. Note  
9 that the time when the maximum increase in surface  $\text{PM}_{2.5}$  concentration occurs is not the  
10 time when the maximum surface  $\text{PM}_{2.5}$  concentration occurs. Averaged during 10–15  
11 January, the diurnal changes in surface  $\text{PM}_{2.5}$  concentration in Fig. 11b, d, and f show  
12 that the increase in surface  $\text{PM}_{2.5}$  concentration starts from 09:00, with values of  $6\text{--}28 \mu\text{g}$   
13  $\text{m}^{-3}$  (10–25%),  $10\text{--}35 \mu\text{g m}^{-3}$  (7–20%),  $10\text{--}35 \mu\text{g m}^{-3}$  (7–15%) for Beijing, Tianjin, and  
14 Hebei, respectively. The surface  $\text{PM}_{2.5}$  concentration is maximum at around 08:00 and  
15 20:00 and minimum during 10:00–16:00, while the maximum increase in surface  $\text{PM}_{2.5}$   
16 concentration occurs at 10:00 and 16:00. The feedback of meteorological variables  
17 change to surface  $\text{PM}_{2.5}$  concentration is significant during 09:00–18:00, and thus  
18 increases the average value and weakens the daily variation of surface  $\text{PM}_{2.5}$   
19 concentration.

20 Figure 12a shows the impact of changes in meteorological variables on the spatial  
21 distribution of surface  $\text{PM}_{2.5}$  concentration averaged during 09:00–18:00, 10–15 January.  
22 Consistent with Fig. 11, the meteorological-variables-change-induced increase of surface  
23  $\text{PM}_{2.5}$  concentration is maximum over Tianjin and south Hebei Province, with values of

1 30–50  $\mu\text{g m}^{-3}$ ; in south Beijing, the values range from 10 to 40  $\mu\text{g m}^{-3}$ . Figure 12b shows  
2 that the corresponding surface  $\text{PM}_{2.5}$  concentration change in percentage terms is higher  
3 over southeast Beijing and north Tianjin with the value of 15–30% while is 2–15% over  
4 south Hebei Province, south Tianjin and north Beijing. It can be concluded that aerosol  
5 induces a more stable atmosphere, which is favorable for the accumulation of air  
6 pollutants, and thus contributes to the formation of fog-haze events. A mechanism of  
7 positive feedback exists between aerosol concentration and aerosol-induced  
8 meteorological conditions.

9

## 10 **5. Conclusion**

11 Heavy particulate pollution and fog-haze events over the NCP have drawn much  
12 attention recently. In this paper, we estimate the feedback between atmospheric aerosols  
13 and meteorological variables during a fog-haze period in January 2013. This is achieved  
14 by conducting numerical simulations using a coupled meteorology and aerosol/chemistry  
15 model (WRF-Chem). The period from 10–15 January, when the NCP experienced a  
16 severe fog-haze event, is analyzed in detail. Major conclusions are as follows.

17 The spatial and temporal characteristics of temperature, RH, wind, surface  $\text{PM}_{2.5}$   
18 concentration, visibility and AOD during 2–26 January 2013 is reproduced by the  
19 simulation using the fully-coupled WRF-Chem model.

20 The results of the numerical experiments show that, averaged during 09:00–18:00,  
21 10–15 January, aerosols lead to a significant negative radiative forcing of  $-20$ – $-140 \text{ W m}^{-2}$   
22 at the surface and a large positive radiative forcing of  $20$ – $120 \text{ W m}^{-2}$  in the atmosphere  
23 and the temperature decreases by  $0.8$ – $2.8 \text{ }^\circ\text{C}$  at the surface and increases by  $0.1$ – $0.5 \text{ }^\circ\text{C}$  at

1 around 925 hPa while the RH increases by about 4–12% at the surface and decreases by  
2 1–6% at around 925 hPa. The maximum change occurs over urban Beijing and Tianjin,  
3 and south Hebei Province. As a result, the aerosol-induced equivalent potential  
4 temperature profile change shows that the atmosphere is much more stable and thus the  
5 surface wind speed decreases by up to  $0.3 \text{ m s}^{-1}$  (10%) and the atmosphere boundary  
6 layer height decreases by 40–200 m (5–30%) during the daytime of this severe fog-haze  
7 event.

8 The results of the numerical experiments also show that, due to such a more stable  
9 atmosphere, compared to the surface  $\text{PM}_{2.5}$  concentration from the model results without  
10 aerosol feedback, the maximum increase of hourly surface  $\text{PM}_{2.5}$  concentration is around  
11  $50 \mu\text{g m}^{-3}$  (70%),  $90 \mu\text{g m}^{-3}$  (60%), and  $80 \mu\text{g m}^{-3}$  (40%) in Beijing, Tianjin, and south  
12 Hebei Province, respectively, during 10–15 January. The surface  $\text{PM}_{2.5}$  concentration  
13 averaged during 09:00–18:00, 10–15 January, over the NCP, increases by  $10\text{--}50 \mu\text{g m}^{-3}$ ,  
14 with the maximum change taking place over urban Beijing and Tianjin, and south Hebei  
15 Province. Although the aerosol concentration is maximum during the nighttime, the  
16 feedback mechanism by which meteorological variables increase the aerosol  
17 concentration most occurs during daytime (at around 10:00 and 16:00). These results  
18 suggest that aerosol induces a more stable atmosphere, which is favorable for the  
19 accumulation of air pollutants, and thus contributes to the formation of fog-haze events.  
20 A mechanism of positive feedback exists between aerosol concentration and aerosol-  
21 induced meteorological conditions.

22 | There are uncertainties in this study. The model overestimates  $\text{PM}_{2.5}$  at Xianghe and  
23 | Tianjin according to Figure 3. The diurnal variation of  $\text{PM}_{2.5}$  at Xianghe and Tianjin from

1 model results and observations shows that the overestimation is basically at night which  
2 may relate to the setting of atmospheric boundary layer height at night in the model and  
3 also the bias of emission inputted to the model. As the aerosol feedback derived from the  
4 aerosol radiative effect mainly has large impacts during daytime, it is noted that the  
5 overestimation of PM<sub>2.5</sub> may lead to slight overestimation of the aerosol feedback during  
6 the pollutant period. Emission with higher resolution may be useful for improving the  
7 model performance. The aerosol direct and indirect effect is also very sensitive to the  
8 mixing state between scattering aerosols and absorbing aerosols. Moreover, the feedback  
9 between aerosol and cloud/meteorological parameters also has large uncertainty.  
10 Although aerosol indirect forcing is considered in WRF-Chem, it only includes the  
11 aerosol effect on resolved stratiform clouds. With a horizontal resolution of 27 km,  
12 convective clouds are still parameterized in the model without explicit cloud  
13 microphysics in the convective cloud parameterization that links aerosols to cloud  
14 condensation or ice nuclei.

## 17 **Acknowledgements**

18 This work was supported by the National Basic Research Program  
19 of China (2014CB953802), the “Strategic Priority Research Program (B)” of the Chinese  
20 Academy of Sciences (XDB05030105, XDB05030102, XDB05030103), the International  
21 S&T Cooperation Program of China (2011DFG23450), the National Natural Science  
22 Foundation of China (41305010) and the Russian Scientific Fund under grant 14-47-  
23 00049.

1 ~~This work was supported by the National~~  
2 ~~Basic Research Program of China (2014CB953802), the “Strategic Priority Research~~  
3 ~~Program (B)” of the Chinese Academy of Sciences (XDB05030105, XDB05030102,~~  
4 ~~XDB05030103), and an NSFC project (41305010).~~

## 8 **References**

9 Abdul-Razzak, H., and Ghan, S.J.: A parameterization of aerosol activation 2. Multiple  
10 aerosol types, *J. Geophys. Res.*, 105(D5), 6837–6844, 2000.

11 Albrecht, B.A.: Aerosols, cloud microphysics, and fractional cloudiness, *Science*, 245,  
12 1227–1230, 1989.

13 Barndard, J.C., Fast, J.D., Paredes-Miranda, G., Arnott, W.P., and Laskin, A.: Technical  
14 Note: Evaluation of the WRF-Chem “Aerosol Chemical to Aerosol Optical Properties”  
15 Module using data from the MILAGRO campaign, *Atmos. Chem. Phys.*, 10, 7325–7340,  
16 2010.

17 Brown, J.F., Loveland, T.R., Merchant, J.W., Reed, B.C., and Ohlen, D.O.: Using multi-  
18 source data in global land-cover characterization: concepts, requirements, and methods,  
19 *Photogram. Eng. Rem. S.*, 59, 977–987, 1993.

20 Chan, C.K., and Yao, X.: Air pollution in mega cities in China, *Atmos. Environ.*, 42, 1–  
21 42, 2008.

22 Che, H., Xia, X., Zhu, J., Li, Z., Dubovik, O., Holben, B., Goloub, P., Chen, H., Estelles,  
23 V., Cuevas-Agulló E., Blarel, L., Wang, H., Zhao, H., Zhang, X., Wang, Y., Sun, J., Tao,  
24 R., Zhang, X., and Shi, G.: Column aerosol optical properties and aerosol radiative  
25 forcing during a serious haze-fog month over North China Plain in 2013 based on  
26 ground-based sunphotometer measurements, *Atmos. Chem. Phys.*, 14, 2125–2138, 2014.

27 [Che, H., Zhang, X., Chen, H., Damiri, B., Goloub, P., Li, Z., Zhang, X., Wei, Y., Zhou, H.,](#)  
28 [Dong, F., Li, D., and Zhou, T.: Instrument calibration and aerosol optical depth validation](#)  
29 [of the China Aerosol Remote Sensing Network, \*J. Geophys. Res.\*, 114, D03206,](#)  
30 [doi:10.1029/2008JD011030, 2009a.](#)

- 1 Che, H., Zhang, X., Li, Y., Zhou, Z., and Qu, J.J.: Horizontal visibility trends in China  
2 1981-2005, *Geophys. Res. Lett.*, 34, L24706, doi:10.1029/2007GL031450, 2007.
- 3 Che, H., Zhang, X., Li, Y., Zhou, Z., Qu, J., and Hao, X.: Haze trends over the capital  
4 cities of 31 provinces in China, 1981-2005, *Theor. Appl. Climatol.*, 97, 235–242, 2009**b**.
- 5 Cheng, S., Yang, L., Zhou, X., Xue, L., Gao, X., Zhou, Y., and Wang, W.: Size-  
6 fractionated water-soluble ions, situ PH and water content in aerosol on hazy days and  
7 the influences on visibility impairment in Jinan, China, *Atmos. Environ.*, 45, 4631–4640,  
8 2011.
- 9 Deng, X. J., Tie, X., Wu, D., Zhou, X. J., Tan, H. B., Li, F., and Jiang, C.: Long-term  
10 trend of visibility and its characterizations in the Pearl River Delta Region (PRD), China,  
11 *Atmos. Environ.*, 42, 1424–1435, 2008.
- 12 Dubovik, O., Holben, B., Eck, T.F., Smirnov, A., Kaufman, Y.J., King, M.D., Tanre, D.,  
13 and Slutsker, I.: Variability of absorption and optical properties of key aerosol types  
14 observed in worldwide locations, *J. Atmos. Sci.*, 59, 590-608, 2002.
- 15 Dubovik, O., and King, M.D.: A flexible inversion algorithm for retrieval of aerosol  
16 optical properties from Sun and sky radiance measurements, *J. Geophys. Res.*, 105,  
17 20673-20696, 2000.
- 18 Fast, J.D., Gustafson, Jr. W.I., Easter, R.C., Zaveri, R.A., Barnard, J.C., Chapman, E.G.,  
19 and Grell, G.A.: Evolution of ozone, particulates, and aerosol direct forcing in an urban  
20 area using anew fully-coupled meteorology, chemistry, and aerosol model, *J. Geophys.*  
21 *Res.*, 111, D21305, doi:10.1029/2005JD006721, 2006.
- 22 Feng, S., Hu, S.Q., and Qian, W.H.: Quality control of daily meteorological data in China,  
23 1951–2000: A new dataset, *Int. J. Climatol.*, 24, 853–870, 2004.
- 24 Gao, Y., and Zhang, M.: Numerical Simulation of a Heavy Fog-Haze Episode over the  
25 North China Plain in January 2013, *Climatic Environ. Res. (in Chinese)*, 19(2), 140–152,  
26 2014.
- 27 Ghan, S.J., Easter, R.C., Hudson, J., and Breon, F.-M.: Evaluation of Aerosol Indirect  
28 Radiative Forcing in MIRAGE, *J. Geophys. Res.*, 106, 5317–5334, 2001a.
- 29 Ghan, S., Laulainen, N., Easter, R., Wagener, R., Nemesure, S., Chapman, E., Zhang, Y.,  
30 and Leung, R.: Evaluation of aerosol direct radiative forcing in MIRAGE, *J. Geophys.*  
31 *Res.*, 106, 5295–5316, 2001b.
- 32 Gong, S.L.: A parameterization of sea-salt aerosol source function for sub- and super-  
33 micron particles, *Global Biogeochem. Cycles*, 17, 1097, doi:10.1029/2003GB002079,  
34 2003.

- 1 Gong, S.L., Barrie, L.A., and Blanchet, J.-P.: Modeling sea-salt aerosols in the  
2 atmosphere, *J. Geophys. Res.*, 102, 3805–3818, 1997.
- 3 Grell, G.A., Peckham, S.E., Schmitz, R., McKeen, S.A., Frost, G., Skamarock, W.C., and  
4 Eder, B.: Fully coupled "online" chemistry within the WRF model, *Atmos. Environ.*, 39,  
5 6957–6975, 2005.
- 6 Guenther, A., Karl, T., Harley, P., Wiedinmyer, C., Palmer, P.I., and Geron, C.:  
7 Estimates of global terrestrial isoprene emissions using MEGAN (Model of Emissions of  
8 Gases and Aerosols from Nature), *Atmos. Chem. Phys.*, 6, 3181–3210, 2006.
- 9 Gustafson, Jr W.I., Chapman, E.G., Ghan, S.J., Easter, R.C., and Fast, J.D.: Impact on  
10 modeled cloud characteristics due to simplified treatment of uniform cloud condensation  
11 nuclei during NEAQS 2004, *Geophys. Res. Lett.*, 34, L19809,  
12 doi:10.1029/2007GL030021, 2007.
- 13 Han, X., Zhang, M., Tao, J., Wang, L., Gao, J., Wang, S., and Chai, F.: Modeling aerosol  
14 impacts on atmospheric visibility in Beijing with RAMS-CMAQ, *Atmos. Environ.*, 72,  
15 177–191, 2013.
- 16 [He, K. B.: Multi-resolution Emission Inventory for China \(MEIC\): model framework and](#)  
17 [1990-2010 anthropogenic emissions, International Global Atmospheric Chemistry](#)  
18 [Conference, 17-21 September, Beijing, China, 2012.](#)
- 19 Holben, B.N., Eck, T.F., Slutsker, I., Tanre, D., Buis, J. P., Setzer, A., Vermote, E.,  
20 Reagan, J.A., Kaufman, Y.J., Nakajima, T., Lavenu, F., Jankowiak, I., and Smirnov, A.:  
21 AERONET--A federated instrument network and data archive for aerosol  
22 characterization, *Remote Sens. Environ.*, 66, 1-16, 1998.
- 23 Hsu, N.C., Jeong, M.J., Bettenhausen, C., Sayer, A.M., Hansell, R., Seftor, C.S., Huang,  
24 J., and Tsay, S.C.: Enhanced Deep Blue aerosol retrieval algorithm: The second  
25 generation, *J. Geophys. Res.*, 118(16), 9296–9315, 2013.
- 26 Huang, Y., Dickinson, R.E., and Chameides, W.L.: Impact of aerosol indirect effect on  
27 surface temperature over East Asia, *Proc. Natl. Acad. Sci.*, 103, 4371–4376,  
28 doi:10.1073/pnas.0504428103, 2006.
- 29 Jaeglé L., Quinn, P.K., Bates, T.S., Alexander, B., and Lin, J.-T.: Global distribution of  
30 sea salt aerosols: new constraints from in situ and remote sensing observations, *Atmos.*  
31 *Chem. Phys.*, 11, 3137–3157, doi:10.5194/acp-11-3137-2011, 2011.
- 32 [Lei, Y., Zhang, Q., He, K.B., and Streets, D.G.: Primary anthropogenic aerosol emission](#)  
33 [trends for China, 1990–2005, \*Atmos. Chem. Phys.\*, 11, 931–954](#)  
34 [<http://dx.doi.org/10.5194/acp-11-931-2011>, 2011.](#)

- 1 Li, Z., Xia, X., Cribb, M., Mi, W., Holben, B., Chen, H., Wang, P., Tsay, S.-C., Eck, T.  
2 F., Zhao, F., Dutton, E.G., and Dickerson, R.E.: Aerosol optical properties and its  
3 radiative effects in northern China, *J. Geophys. Res.*, 112, D22S01,  
4 doi:10.1029/2006JD007382, 2007.
- 5 Liu, H., Zhang, L., and Wu, J.: A Modeling Study of the Climate Effects of Sulfate and  
6 Carbonaceous Aerosols over China, *Adv. Atmos. Sci.*, 27, 1276–1288, 2010.
- 7 Liu, J., Xia, X., Wang, P., Li, Z., Zheng, Y., Cribb, M. and Chen, H.: Significant aerosol  
8 direct radiative effects during a pollution episode in northern China, *Geophys. Res. Lett.*,  
9 34, L23808, doi:10.1029/2007GL030953, 2007.
- 10 Liu, Y., Daum, P.H., and McGraw, R.: Size Truncation Effect, Threshold Behavior, and a  
11 New Type of Autoconversion Parameterization, *Geophys. Res. Lett.*, 32, L11811,  
12 doi:10.1029/2005GL022636, 2005.
- 13 Loveland, T.R., Merchant, J.W., Ohlen, D.O., and Brown, J.F.: Development of a land-  
14 cover characteristics database for the conterminous US, *Photogram. Eng. Rem. S.*, 57,  
15 1453–1463. 1991.
- 16 Patashnick, H, and Rupprecht, E.: Continuous PM10 measurements using the tapered  
17 element oscillating microbalance, *J Air Waste Manage.*, 41, 1079–1083. 1991.
- 18 Petters, M.D., and Kreidenweis, S.M.: A single parameter representation of hygroscopic  
19 growth and cloud condensation nucleus activity, *Atmos. Chem. Phys.*, 7, 1961–1971,  
20 doi:10.5194/acp-7-1961-2007, 2007.
- 21 Qian, Y., Leung, L.R., Ghan, S.J., and Giorgi, F.: Regional climate effects of aerosols  
22 over China: Modeling and observation, *Tellus B*, 515, 914–934, 2003.
- 23 Quan, J., Zhang, Q., He, H., Liu, J., Huang, M., and Jin, H.: Analysis of the formation of  
24 fog and haze in North China Plain (NCP), *Atmos. Chem. Phys.*, 11, 8205-8214,  
25 doi:10.5194/acp-11-8205-2011, 2011.
- 26 Ramanathan, V., Crutzen, P.J., Kiehl, J.T., and Rosenfeld, D.: Aerosols, climate, and the  
27 hydrological cycle, *Science* 294, 2119–2124, 2001.
- 28 Randerson, J.T., Van der Werf, G.R., Giglio, L., Collatz, G.J., and Kasibhatla, P.S.:  
29 Global Fire Emissions Database, Version 2 (GFEDv2.1). Available at  
30 <http://daac.ornl.gov/> (last access: 11 November 2013) from Oak Ridge National  
31 Laboratory Distributed Active Archive Center, Oak Ridge, Tennessee, USA,  
32 doi:10.3334/ORNLDAAAC/849, 2005.
- 33 Skamarock, W.C., Klemp, J.B., Dudhia, J., Gill, D.O., Barker, D.M., Duda, M., Huang,  
34 X.-Y., Wang, W., and Powers, J.G.: A description of the Advanced Research WRF  
35 version 3.Tech. Rep. NCAR/TN-475+STR, 113 pp, 2008, Boulder, Colorado, USA.

- 1 Streets, D.G., Bond, T.C., Carmichael, G.R., Fernandes, S.D., Fu, Q., He, D., Klimont, Z.,  
2 Nelson, S.M., Tsai, N.Y., Wang, M.Q., Woo, J.-H., and Yarber, K.F.: An inventory of  
3 gaseous and primary aerosol emissions in Asia in the year 2000, *J. Geophys. Res.*  
4 108(D21), 8809, doi:10.1029/2002JD003093, 2003.
- 5 Sun, Y., Jiang, Q., Wang, Z., Fu, P., Li, J., Yang, T., and Yin, Y.: Investigation of the  
6 Sources and Evolution Processes of Severe Haze Pollution in Beijing in January 2013, *J.*  
7 *Geophys. Res.* 114(7), 4380–4398, 2014.
- 8 Sun, Y., Zhuang, G., Tang, A., Wang, Y., and An, Z.: Chemical characteristics of PM<sub>2.5</sub>  
9 and PM<sub>10</sub> in Haze-Fog episodes in Beijing, *Environ. Sci. Technol.*, 40, 3148–3155, 2006.
- 10 Tao, M., Chen, L., Xiong, X., Zhang, M., Ma, P., Tao, J., and Wang, Z.: Formation  
11 process of the widespread extreme haze pollution over northern China in January 2013:  
12 implications for regional air quality and climate, *Atmos. Environ.*, 98, 417–425, doi:  
13 10.1016/j.atmosenv.2014.09.026, 2014.
- 14 Twomey, S.: Pollution and the planetary albedo, *Atmos. Environ.*, 8, 1251–1256, 1974.
- 15 Wang, H., Tan, S.C., Wang, Y., Jiang, C., Shi, G.Y., Zhang, M.X., and Che, H.Z.: A  
16 multisource observation study of the severe prolonged regional haze episode over eastern  
17 China in January 2013, *Atmos. Environ.*, 89, 807–815, 2014b.
- 18 Wang, Y.S., Yao, L., Wang, L.L., Liu, Z., Ji, D., Tang, G., Zhang, J., Sun, Y., Hu, B.,  
19 and Xin, J.: Mechanism for the formation of the January 2013 heavy haze pollution  
20 episode over central and eastern China, *Sci. China Earth Sci.*, 57, 14–25, doi:  
21 10.1007/s11430-013-4773-4, 2014a.
- 22 Wang, S., Zhao, M., Xing, J., Wu, Y., Zhou, Y., Lei, Y., He, K., Fu, L., and Hao, J.:  
23 Quantifying the air pollutants emission reduction during the 2008 Olympic games in  
24 Beijing, *Environ. Sci. Technol.*, 44, 2490–2496, 2010.
- 25 Wu, J., Fu, C., Xu, Y., Tang, J., Han, Z. and Zhang, R.: Effects of total aerosol on  
26 temperature and precipitation in East Asia, *Clim. Res.*, 40, 75–87, 2009.
- 27 Wu, P., and Han, Z.: Indirect radiative and climatic effects of sulfate and organic carbon  
28 aerosols over East Asia investigated by RIEMS, *Atmos. Oceanic Sci. Lett.*, 4, 7–11, 2011.
- 29 Xia, X., Li, Z., Wang, P., Chen, H., and Cribb, M.: Estimation of aerosol effects on  
30 surface irradiance based on measurements and radiative transfer model simulations in  
31 northern China, *J. Geophys. Res.*, 112, D22S10, doi:10.1029/2006JD008337, 2007.
- 32 Yu, M., Carmichael, G.R., Zhu, T., Cheng Y.F.: Sensitivity of predicted pollutant levels  
33 to urbanization in China, *Atmos. Environ.*, 60, 544–554, 2012.

- 1 Zaveri, R.A., Easter, R.C., Fast, J.D., and Peters, L.K.: Model for simulating aerosol  
2 interactions and chemistry (MOSAIC), *J. Geophys. Res.*, 113, D13204,  
3 doi:10.1029/2007JD008792, 2008.
- 4 Zhang, J.K., Sun, Y., Liu, Z.R., Ji, D.S., Hu, B., Liu, Q., Wang, Y.S.: Characterization of  
5 submicron aerosols during a month of serious pollution in Beijing, 2013, *Atmos. Chem.*  
6 *Phys.*, 14 (6), 2887–2903, 2014.
- 7 Zhang, Q., Streets, D.G., Carmichael, G.R., He, K., Huo, H., Kannari, A., Klimont, Z.,  
8 Park, I.S., Reddy, S., Fu, J.S., Chen, D., Duan, L., Lei, Y., Wang, L., and Yao, Z.: Asian  
9 emissions in 2006 for the NASA INTEX-B mission, *Atmos. Chem. Phys.*, 9, 5131–5153,  
10 2009.
- 11 Zhang, X., Wang, Y., Niu, T., Zhang, X., Gong, S., Zhang, Y., and Sun, J.: Atmospheric  
12 aerosol compositions in China: Spatial/temporal variability, chemical signature, regional  
13 haze distribution and comparisons with global aerosols, *Atmos. Chem. Phys.*, 12, 779–  
14 799, doi:10.5194/acp-12-779-2012, 2012.
- 15 Zhao, C., Liu, X., Leung, L.R., and Hagos, S.: Radiative impact of mineral dust on  
16 monsoon precipitation variability over West Africa, *Atmos. Chem. Phys.*, 11, 1879–1893,  
17 2011.
- 18 Zhao, C., Liu, X., Leung, L.R., Johnson, B., McFarlane, S.A., Gustafson, Jr W.I., Fast,  
19 J.D., and Easter, R.C.: The spatial distribution of mineral dust and its shortwave radiative  
20 forcing over North Africa: modeling sensitivities to dust emissions and aerosol size  
21 treatments, *Atmos. Chem. Phys.*, 10, 8821–8838, 2010.
- 22 Zhao, X.J., Zhao, P.S., Xu, J., Meng, W., Pu, W.W., Dong, F., He, D., and Shi, Q.F.:  
23 Analysis of a winter regional haze event and its formation mechanism in the North China  
24 Plain, *Atmos. Chem. Phys.*, 13, 5685–5696, 2013.

25

26

27

28

29

30

31

32

1 Table 1. Statistics of the comparisons between simulated and observed temperature ( $^{\circ}\text{C}$ ),  
 2 relative humidity (RH, %), wind speed ( $\text{m s}^{-1}$ ), surface  $\text{PM}_{2.5}$  concentration ( $\mu\text{g m}^{-3}$ ),  
 3 visibility (km), and aerosol optical depth (AOD) during 2–26 January 2013.

		<sup>a</sup> N	<sup>b</sup> C <sub>OBS</sub>	<sup>b</sup> C <sub>MOD</sub>	<sup>c</sup> R	<sup>d</sup> MB	<sup>d</sup> NMB(%)	<sup>e</sup> RMSE
Temperature	BJ	25	-5.0	-5.5	0.78	-0.5	9.0	1.6
	MY	25	-7.7	-7.6	0.91	0.1	-2.0	1.3
	BD	25	-6.5	-6.0	0.86	0.5	-7.2	1.3
	TS	25	-7.7	-7.6	0.91	0.1	-0.7	1.3
	TJ	25	-5.3	-6.9	0.88	-1.6	31.2	2.1
	QHD	25	-7.9	-7.6	0.83	0.3	-3.4	1.5
RH	BJ	25	57.6	57.1	0.72	-0.4	-0.7	12.6
	MY	25	64.3	63.6	0.84	-0.7	-1.0	10.5
	BD	25	77.5	69.1	0.87	-8.4	-10.8	11.0
	TS	25	70.9	69.9	0.76	-1.0	-1.4	9.6
	TJ	25	64.2	74.4	0.90	10.3	16.0	12.8
	QHD	25	67.5	71.7	0.78	4.1	6.1	8.8
WS	BJ	25	1.7	2.2	0.82	0.5	27.8	0.82
	MY	25	1.6	2.8	0.64	1.2	78.7	1.4
	BD	25	1.8	2.6	0.83	0.75	40.8	1.0
	TS	25	2.1	3.1	0.68	1.0	46.4	1.3
	TJ	25	2.2	2.9	0.65	0.7	30.9	1.2
	QHD	25	2.0	3.8	0.51	1.9	100.0	2.1
PM <sub>2.5</sub>	BJ	600	138.4	123.4	0.63	-15.1	-10.9	102.8
	XL	590	49.1	62.0	0.69	12.9	26.2	44.8
	XH	502	139.8	181.2	0.56	41.4	29.6	113.9
	TJ	500	135.9	216.9	0.69	80.9	59.5	124.9
Visibility	BJ	100	11.2	16.2	0.77	5.0	44.5	10.3
	TJ	100	8.0	8.1	0.66	0.1	0.95	6.0
	BD	100	6.5	7.2	0.58	0.7	10.5	5.8
	SJZ	100	5.8	5.7	0.43	-0.1	-2.8	5.1
AOD	BJ	22	0.52	0.42	0.59	-0.10	-20.2	0.34
	XL	12	0.23	0.34	0.99	0.11	47.2	0.12
	XH	16	0.64	0.41	0.60	-0.23	-36.7	0.47
	Huimin	18	0.96	0.73	0.74	-0.22	-23.3	0.50

4 <sup>a</sup> *N* is the number of paired samples;

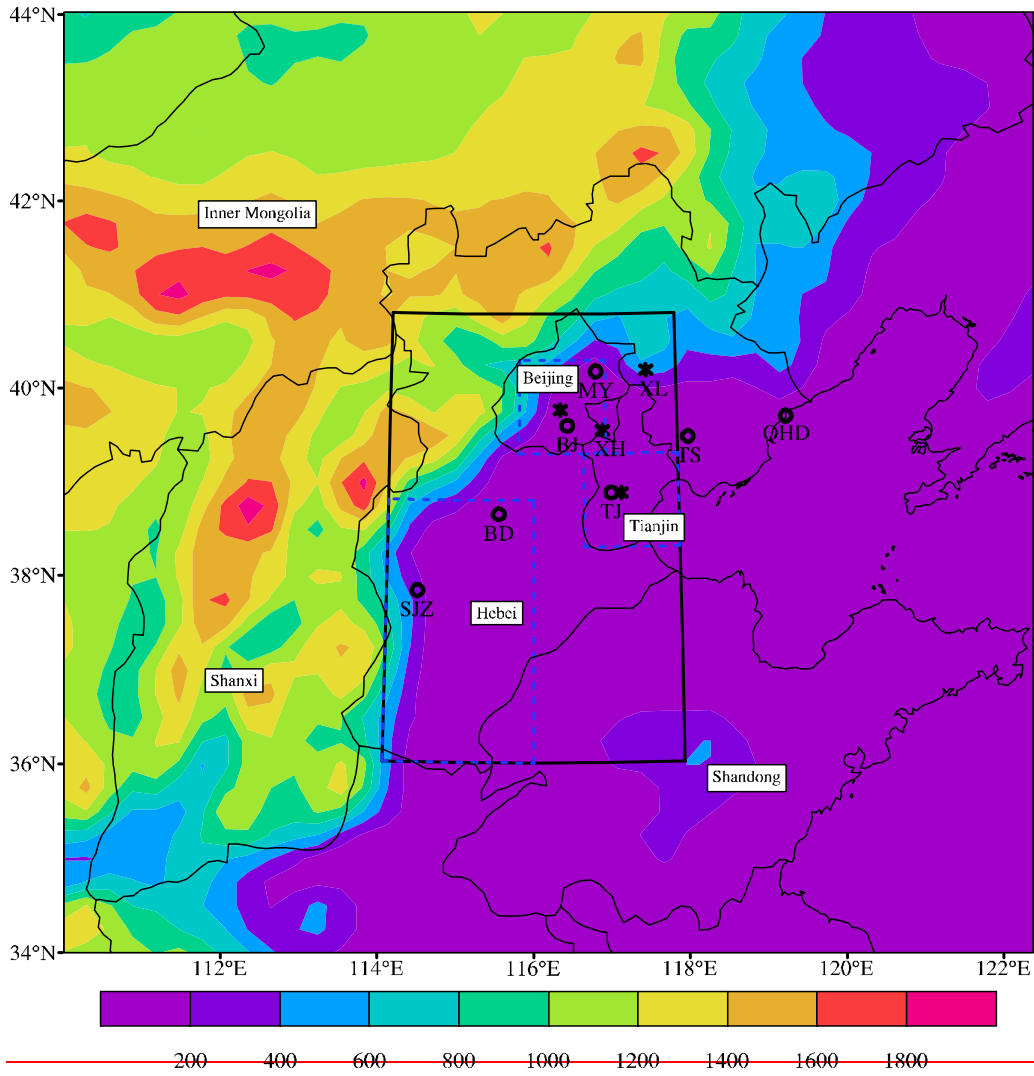
5 <sup>b</sup> *C*<sub>OBS</sub> and *C*<sub>MOD</sub> are the monthly average values of observation and model results,  
 6 sampled at the observation site and time, respectively;

7 <sup>c</sup> *R* is the correlation coefficient between the observation and model results;

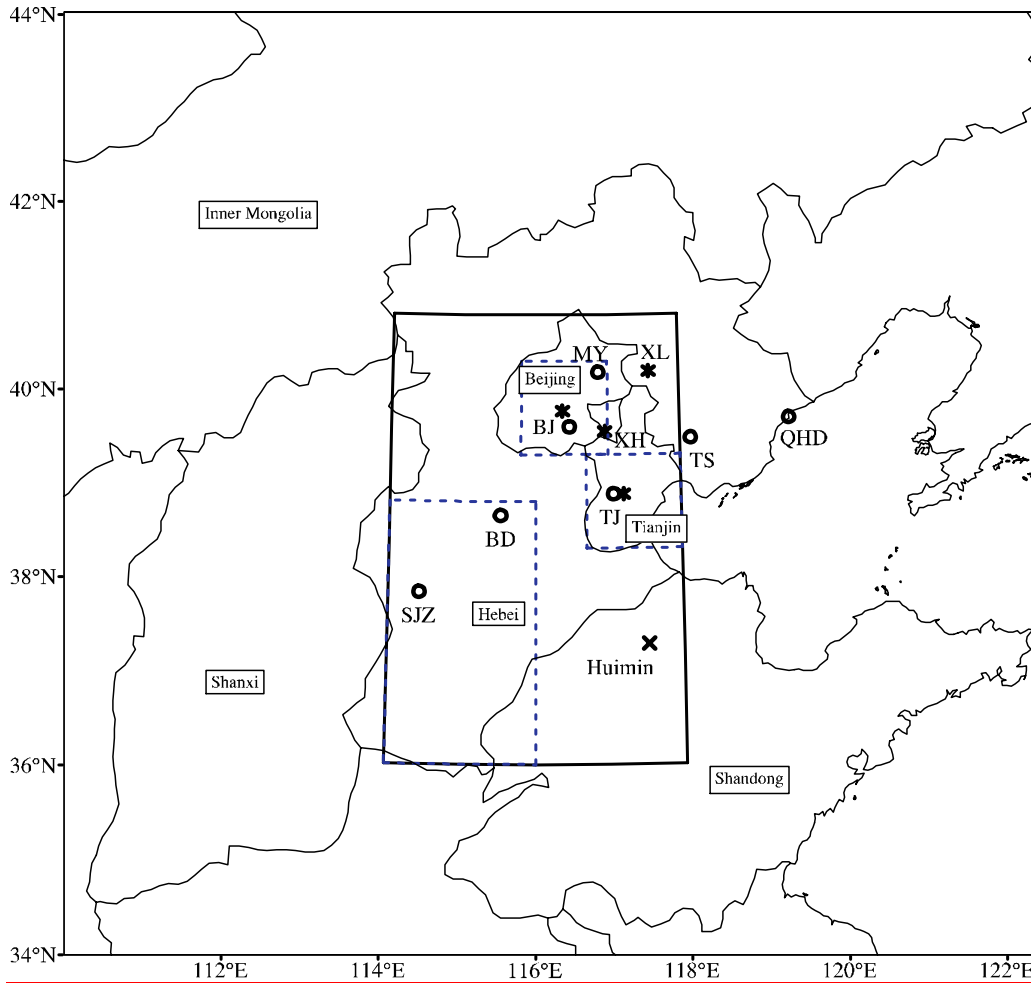
8 <sup>d</sup> *MB* and *NMB* are the mean biases between the observation and model results, and the  
 9 normalized mean bias between the observation and model results, respectively;

10 <sup>e</sup> *RMSE* is the root-mean-square error between observation and model results.

11  
 12



1



1

2 Figure 1. Study domain and ~~the distribution of terrain height and~~ regional divisions:

3 Hebei Province, Beijing, Tianjin, Inner Mongolia, Shanxi Province, and Shandong

4 province. The observation sites (BJ, MY, BD, TS, TJ, QHD and SJZ) from CNMC are

5 denoted as circles and those from the CARE-China network (BJ, TJ, XH and XL) are

6 denoted as stars, of which BJ and TJ from CNMC and the CARE-China network are very

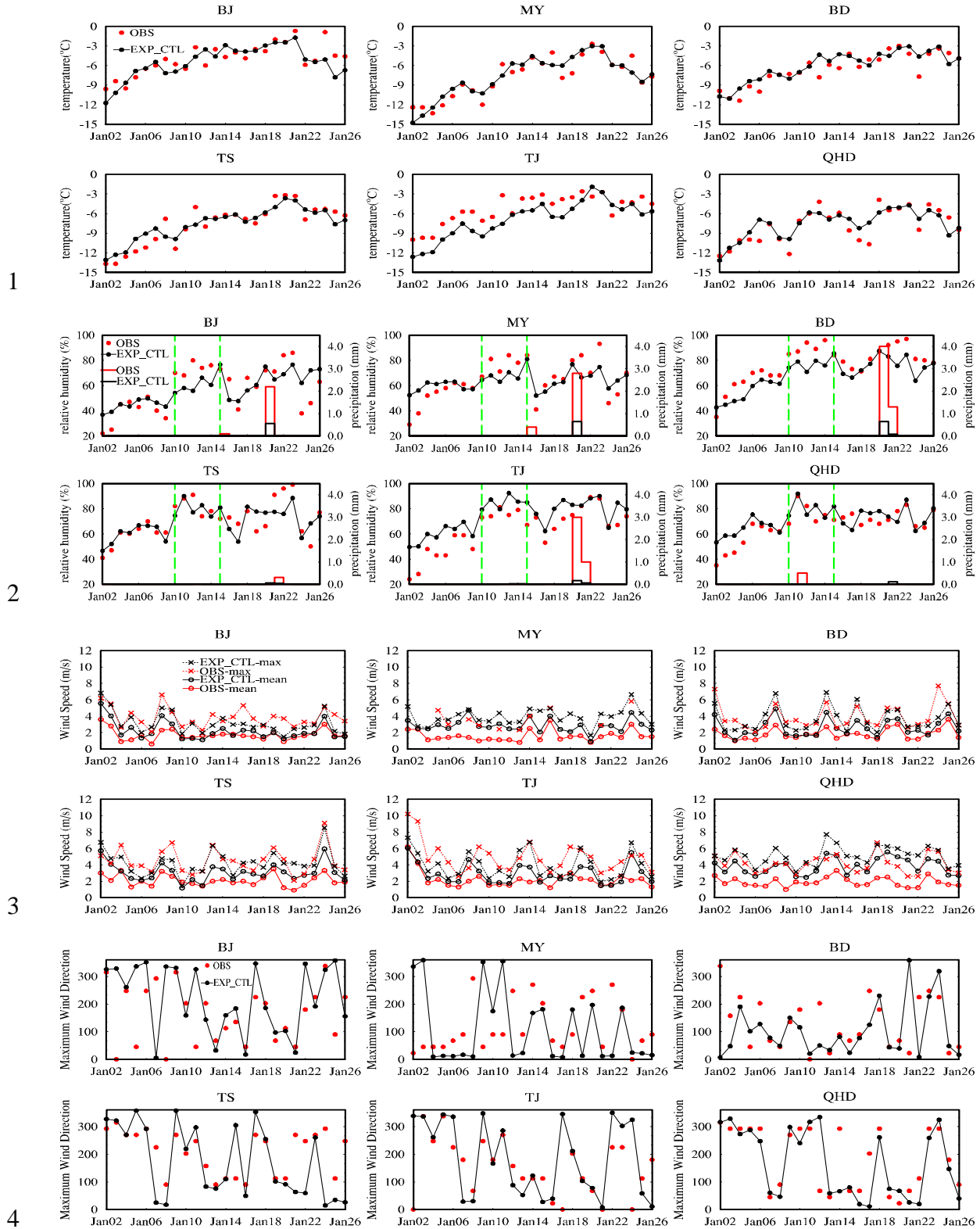
7 close. The observation sites (BJ, XL and XH) from AERONET have the same locations

8 as those from CARE-China. Huimin site from Che et al. (2014) is denoted as a cross. The

9 black box denotes the region of Beijing, Tianjin and Hebei Province (BTH region, 36.2°–

10 41°N, 114°–118°E), and the three blue boxes with dashed lines denote Beijing, Tianjin

11 and south Hebei Province, respectively.



5 Figure 2. Time series of observed (red) and simulated (black, EXP\_CTL) daily-averaged  
 6 2m temperature ( °C), daily-averaged 2m relative humidity (%), daily precipitation (mm,

1 bar), daily-averaged 10m wind speed ( $\text{m s}^{-1}$ , solid line), daily 10m maximum wind speed  
2 (dashed line) and daily wind direction of maximum wind speed at BJ, MY, BD, TS, TJ  
3 and QHD during 2–26 January 2013.

4

5

6

7

8

9

10

11

12

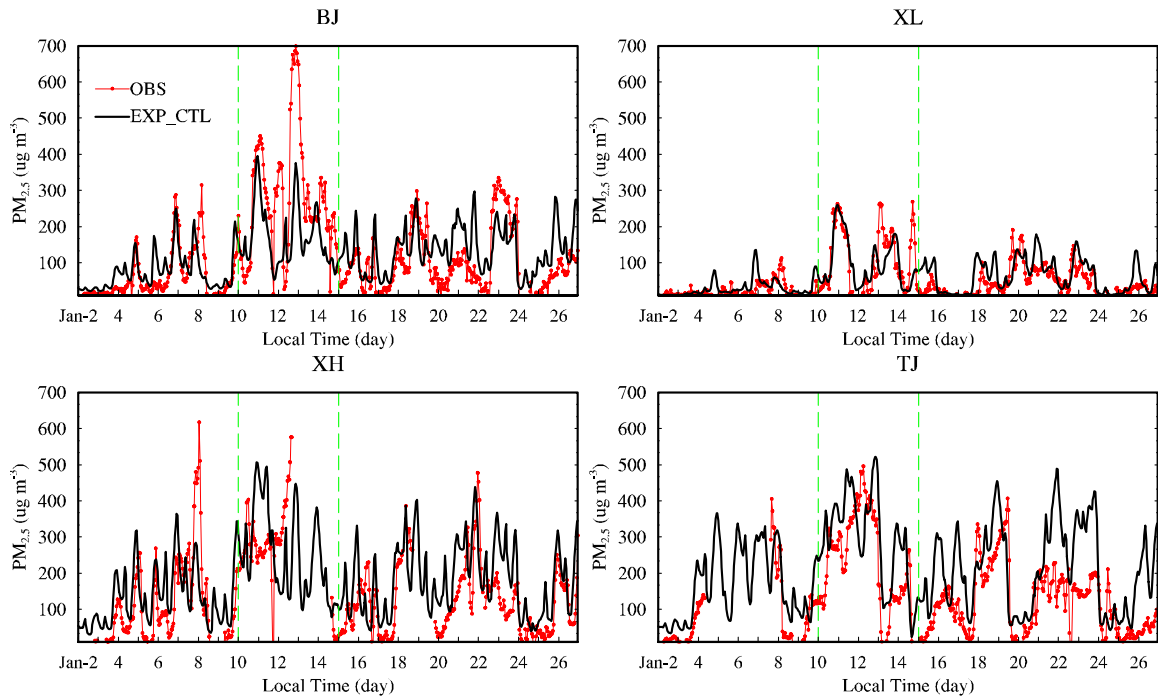
13

14

15

16

17



1

2 Figure 3. Time series of hourly surface PM<sub>2.5</sub> concentration (µg m<sup>-3</sup>) from the CARE-  
 3 China network measurement and the corresponding WRF-Chem simulation (EXP\_CTL)  
 4 at BJ, XL, XH and TJ during 2–26 January 2013.

5

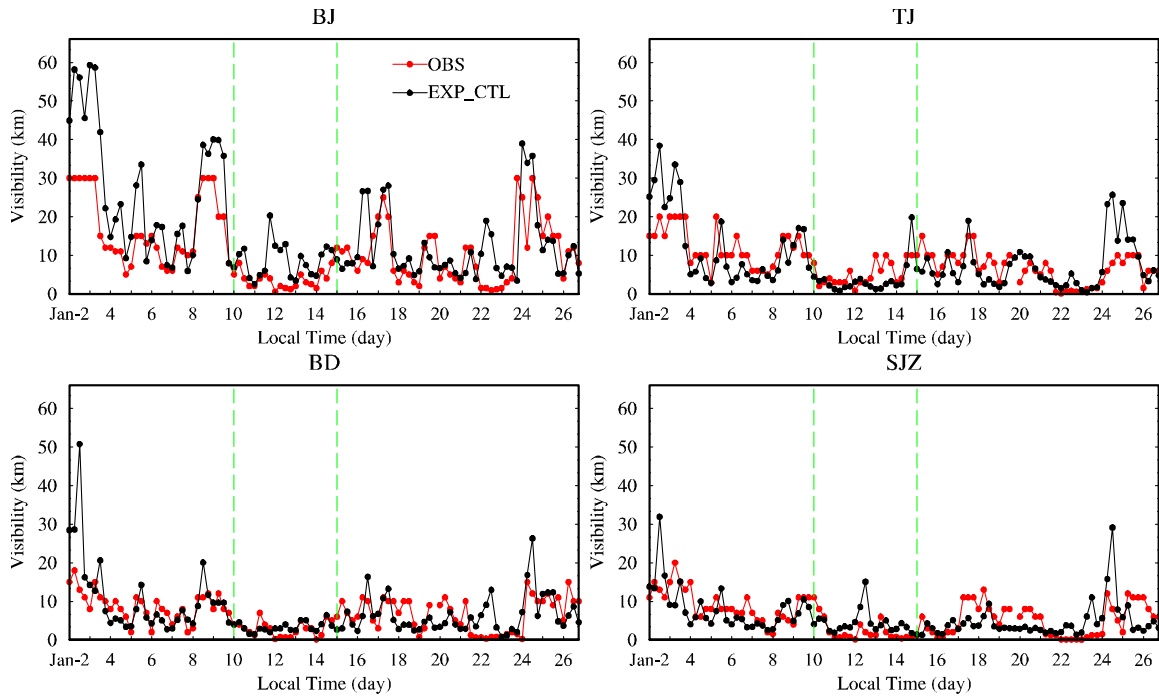
6

7

8

9

10



1

2 Figure 4. Time series of hourly visibility (km) at 00:00, 06:00, 12:00, 18:00 from CNMC  
 3 measurements and the corresponding WRF-Chem simulation (EXP\_CTL) at BJ, TJ, BD  
 4 and SJZ during 2–26 January 2013.

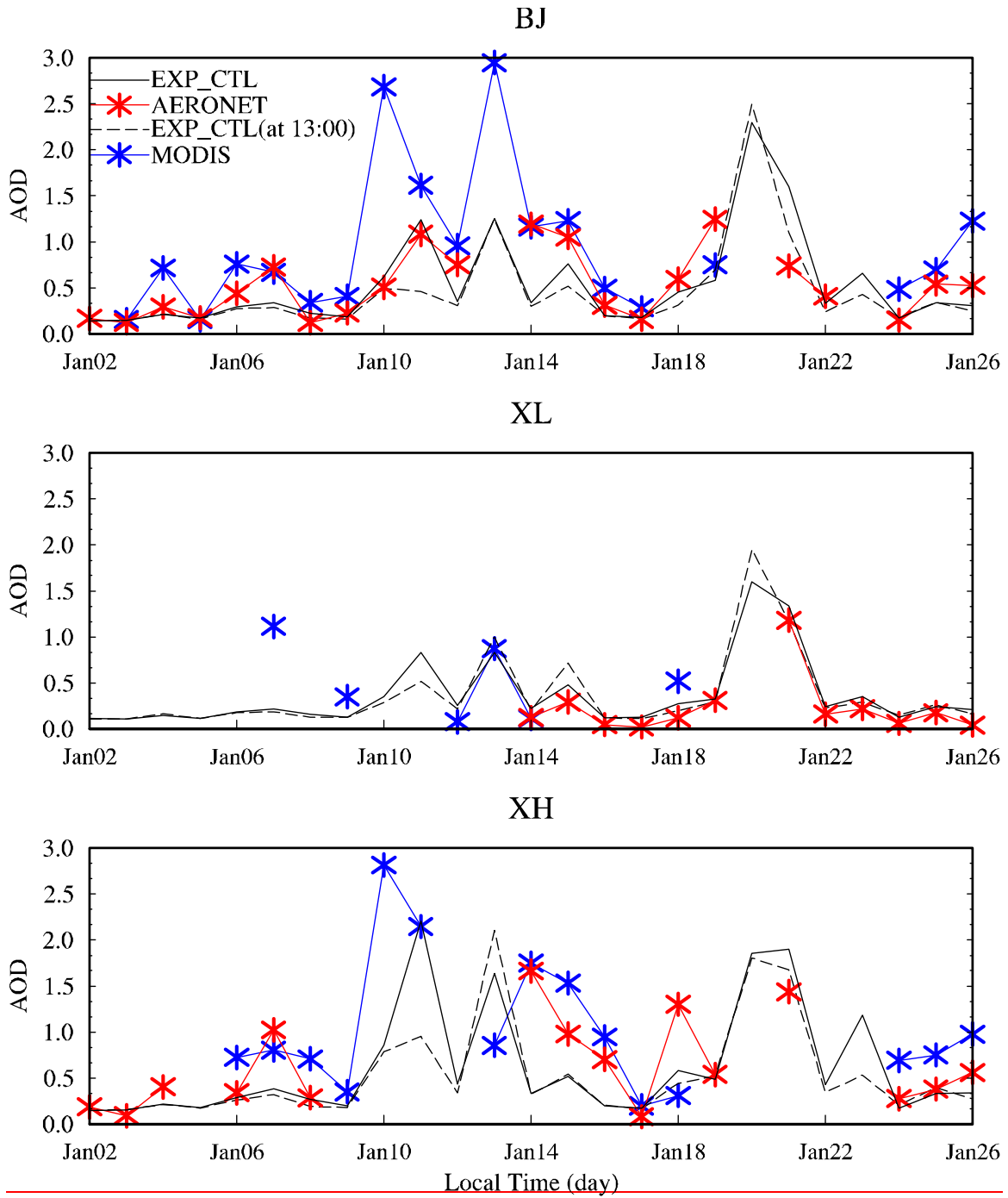
5

6

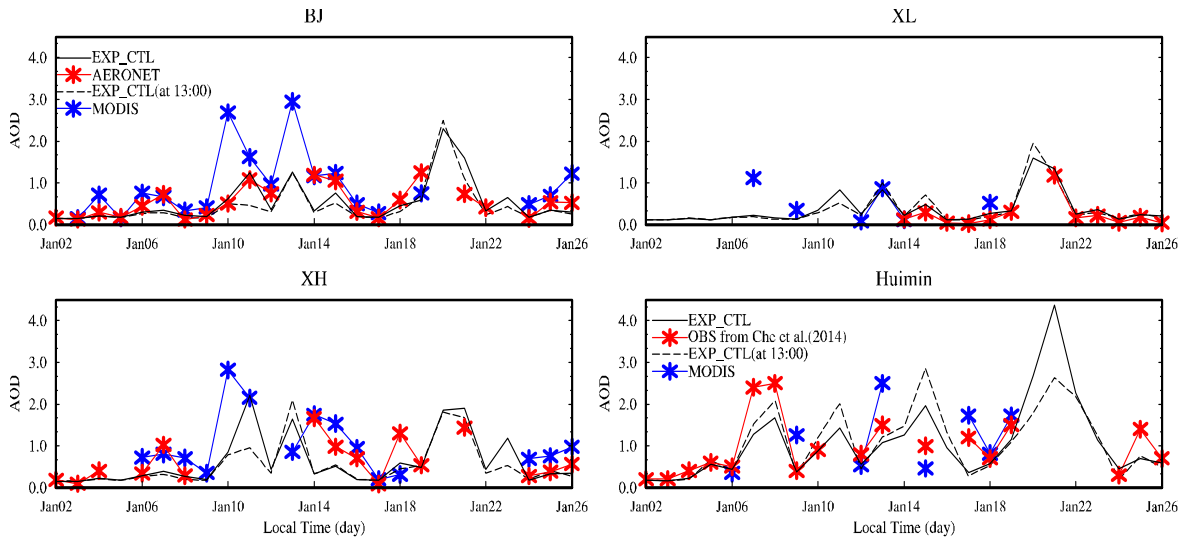
7

8

9



1



1

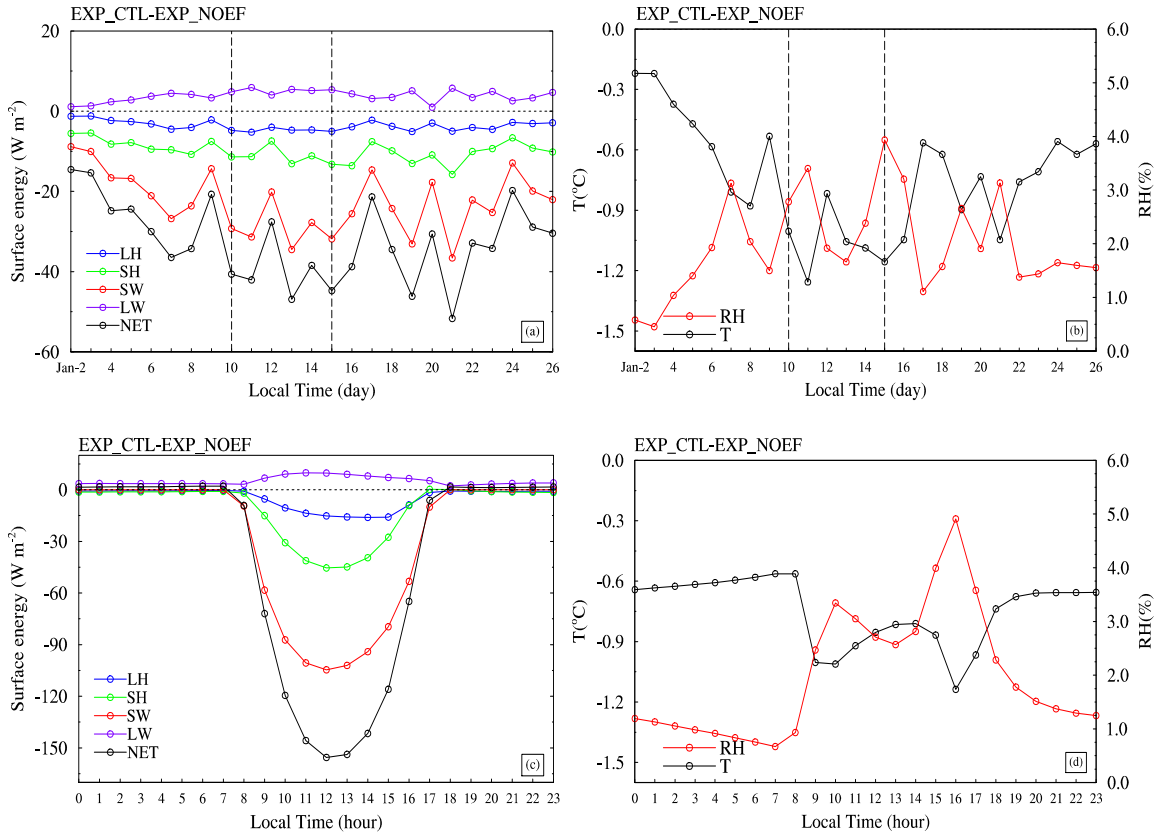
2 Figure 5. Time series of daily AOD at 550 nm from AERONET measurements (~~daily~~  
 3 average) at BJ, XL and XH site and from Che et al. (2014) at Huimin site (daily average)

4 and MODIS retrievals (at 13:00 local time) and the corresponding WRF-Chem  
 5 simulation (EXP\_CTL) for daily average (solid black line) and at 13:00 local time (dash

6 black line) ~~at BJ, XL and XH site~~ during 2–26 January 2013.

7

8



1

2

3

4

5

6

7

8

9

10

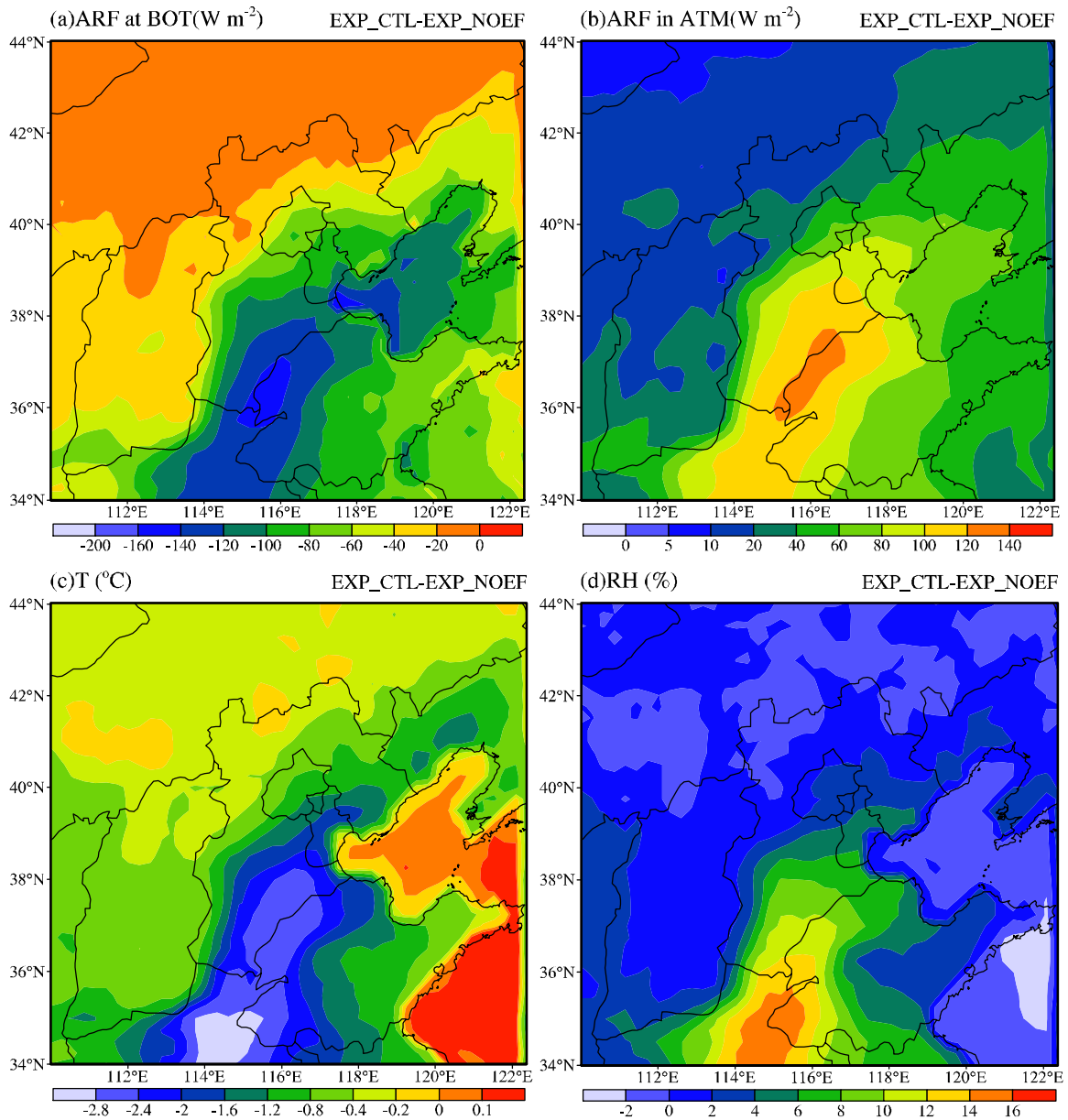
11

12

13

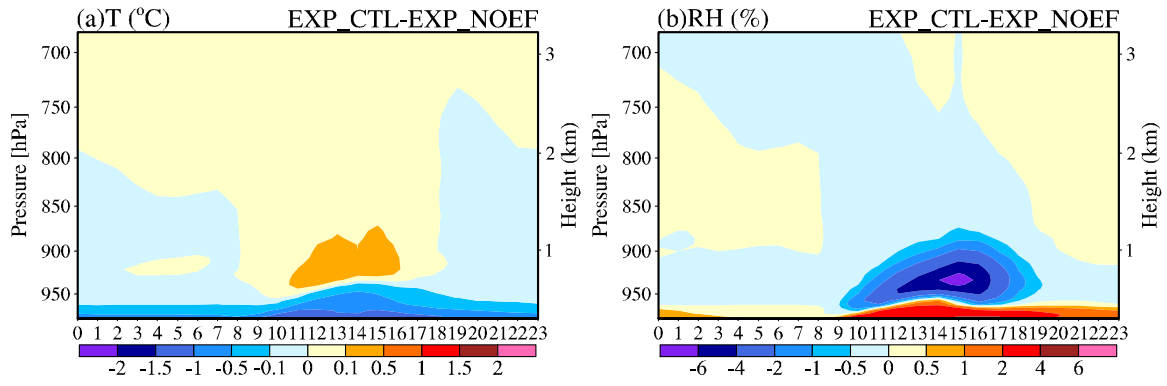
14

Figure 6. Time series of aerosol-induced daily change in (a) surface energy budget (SH, LH, LW radiation, SW radiation, and net radiation energy flux,  $W m^{-2}$ ) and (b) meteorological variables [2m temperature ( $^{\circ}C$ ), 2m RH(%)] averaged for the BTH region ( $36^{\circ}$ – $42^{\circ}N$ ,  $113^{\circ}$ – $120^{\circ}E$ ) during 2–26 January. Time series of aerosol-induced diurnal change of (c) surface energy budget and (d) meteorological variables averaged for the BTH region and the period 10–15 January 2013. LH is latent heat, LW is longwave radiation, SH is sensible heat, SW is shortwave radiation, and NET is the sum of the total energy fluxes.



1  
 2 Figure 7. Spatial distribution of aerosol radiative forcing (ARF,  $W m^{-2}$ ) (a) at bottom and  
 3 (b) in the atmosphere and the aerosol-induced change in (c) 2m temperature ( $^{\circ}C$ ) and (d)  
 4 2m RH (%) averaged during 09:00–18:00, 10–15 January 2013.

5



1

2 Figure 8. Time–altitude distribution of aerosol-induced diurnal change in (a) temperature

3 (°C) and (b) RH (%) averaged for the BTH region and the period 10–15 January 2013.

4

5

6

7

8

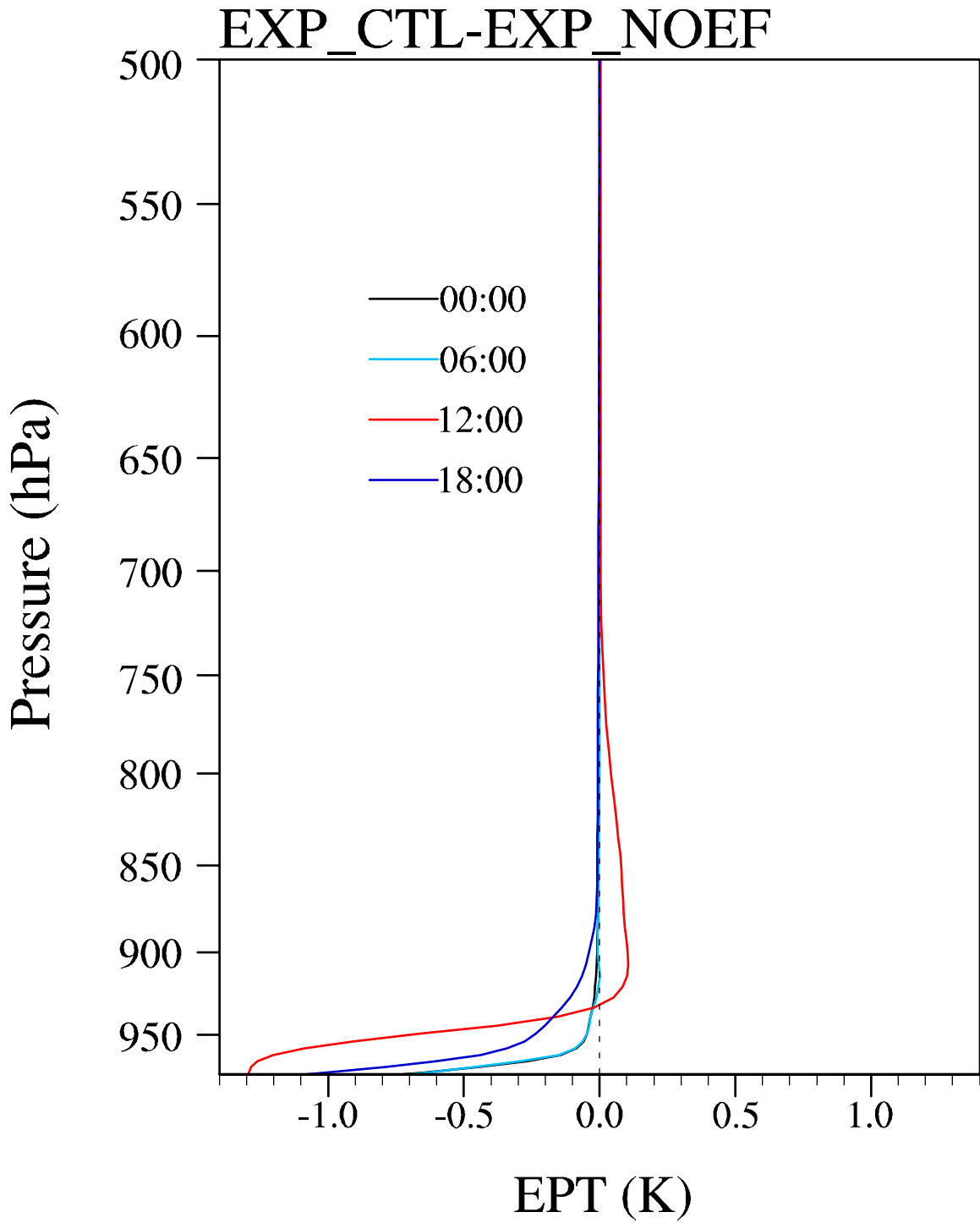
9

10

11

12

13

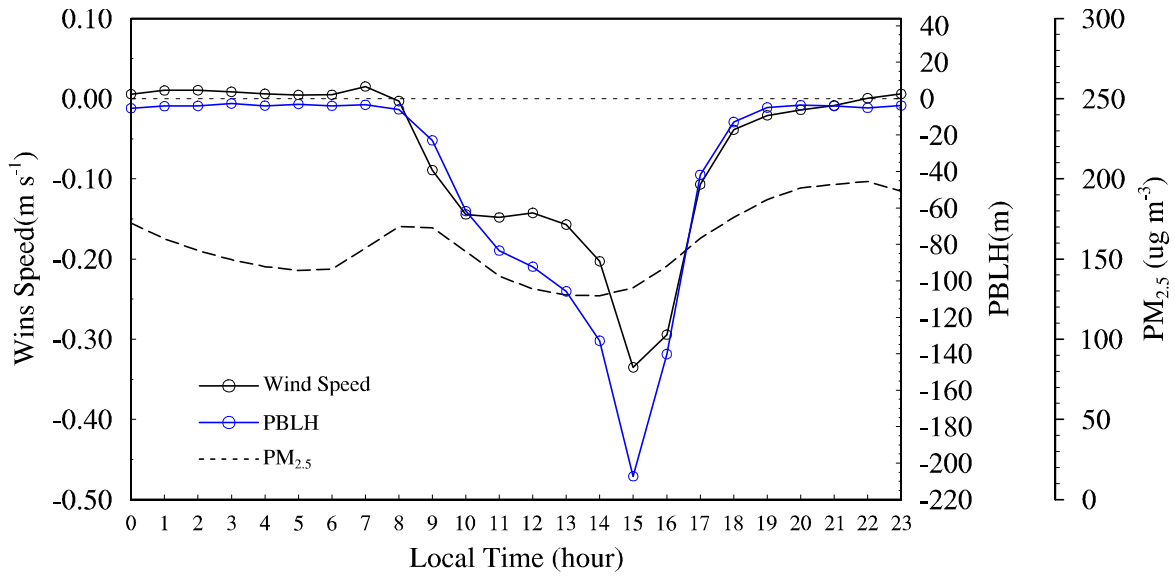


1

2 Figure 9. Aerosol impact on equivalent potential temperature (EPT, K) profiles at 00:00,

3 06:00, 12:00 and 18:00 averaged for the BTH region and the period 10–15 January 2013.

4



1

2 Figure 10. Time series of diurnal variation of surface PM<sub>2.5</sub> concentration from  
 3 EXP\_CTL and aerosol-induced diurnal change of wind speed (m s<sup>-1</sup>) and PBLH (m)  
 4 averaged for the BTH region and the period 10–15 January 2013.

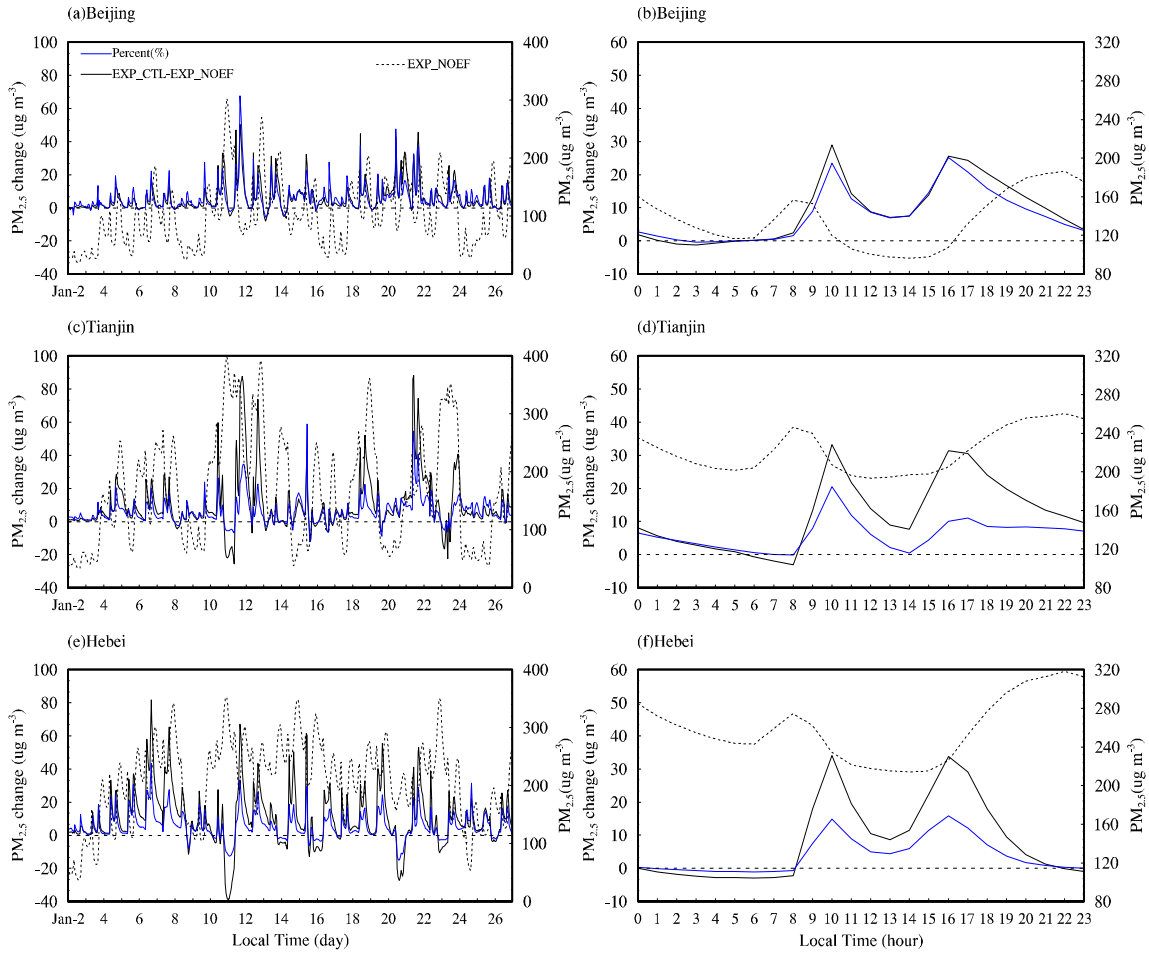
5

6

7

8

9

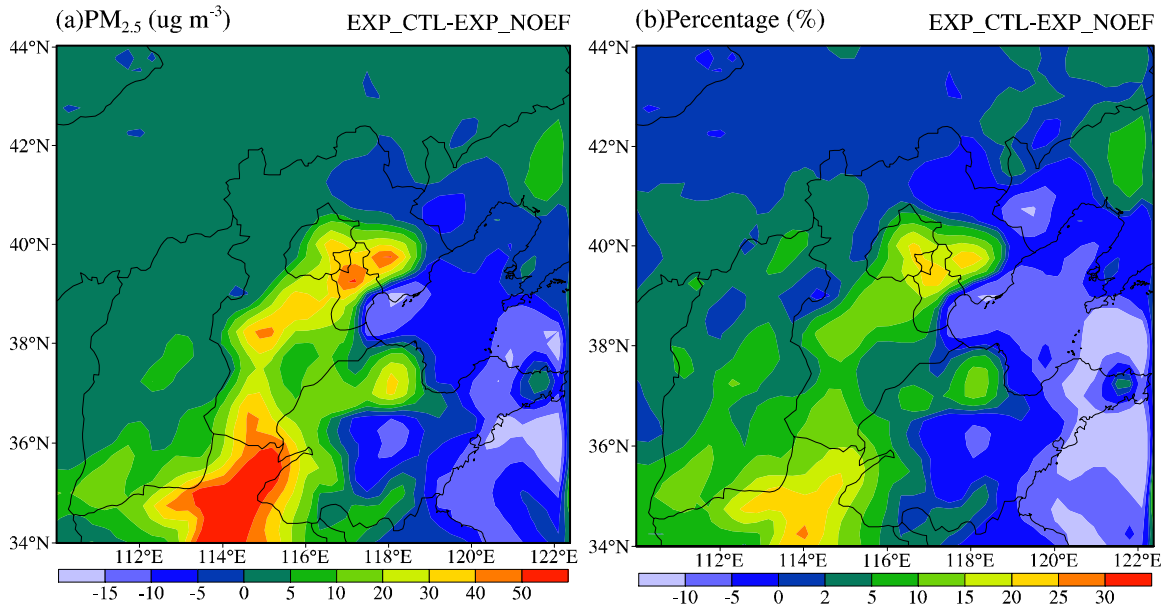


1

2 Figure 11. Time series of surface PM<sub>2.5</sub> concentration from EXP\_NOEF and the  
 3 meteorological-variables-change-induced hourly surface PM<sub>2.5</sub> concentration ( $\mu\text{g m}^{-3}$ )  
 4 change averaged for (a) Beijing, (c) Tianjin and (e) Hebei during 2–26 January and the  
 5 corresponding diurnal change averaged for (b) Beijing, (d) Tianjin and (f) Hebei during  
 6 10–15 January 2013. The black solid line denotes the change value of surface PM<sub>2.5</sub>  
 7 concentration and the blue solid line denotes the corresponding change in percentage  
 8 terms compared to the surface PM<sub>2.5</sub> concentration from the model results of EXP\_NOEF.  
 9 Beijing, Tianjin and Hebei comprise the BTH region (dashed blue boxes in Figure 1).

10

11



1

2 Figure 12. (a) Spatial distribution of the meteorological-variables-change-induced surface

3  $PM_{2.5}$  concentration change ( $\mu g m^{-3}$ ) averaged during 09:00–18:00, 10–15 January 2013.

4 Panel (b) shows the change in percentage terms compared to the surface  $PM_{2.5}$

5 concentration from the model results of EXP\_NOEF.

6

7

8